ADP-15-26-T928
KA-TP-17-2015

Exploring the CP-violating NMSSM: EDM Constraints and Phenomenology

S. F. King[1]*, M. Mühlleitner[2]†, R. Nevzorov[3]‡, K. Walz[2]§

[1] *Physics and Astronomy, University of Southampton, Southampton, SO17 1BJ, U.K.*

[2] *Institute for Theoretical Physics, Karlsruhe Institute of Technology, 76128 Karlsruhe, Germany.*

[3] *ARC Centre of Excellence for Particle Physics at the Tera-scale, School of Chemistry and Physics, University of Adelaide, Adelaide, SA 5005, Australia.*

Abstract

The Next-to-Minimal Supersymmetric extension of the Standard Model (NMSSM) features extra new sources for CP violation. In contrast to the MSSM CP violation can already occur at tree level in the Higgs sector. We investigate the range of possible allowed CP-violating phases by taking into account the constraints arising from the measurements of the Electric Dipole Moments (EDMs) and the latest LHC Higgs data. Our analysis shows that large CP-violating phases, that are NMSSM-specific, are not in conflict with the EDMs. They are dominantly constrained by the Higgs data in this case. We use our results to investigate the prospects of measuring CP violation through the combined measurement of Higgs rates, on the one hand, and in observables based on CP-violating Higgs couplings to tau leptons on the other hand.

*E-mail: king@soton.ac.uk
†E-mail: margarete.muehlleitner@kit.edu
‡E-mail: roman.nevzorov@adelaide.edu.au
§E-mail: kathrin.walz@kit.edu

1 Introduction

The discovery of a Standard Model (SM)-like Higgs boson with mass around 125 GeV by the Large Hadron Collider experiments ATLAS and CMS [1, 2] represents a milestone for particle physics. This discovery supports the Higgs mechanism which allows for the generation of particle masses without violating the underlying gauge symmetries of the SM. It has long been realized that the maximum allowed symmetry compatible with space-time symmetry is supersymmetry (SUSY) [3], which relates bosonic and fermionic degrees of freedom. Due to this and many other virtues as well, SUSY has become one of the most popular and most intensely studied symmetries beyond the SM (BSM). While so far no direct sign of new physics has been found, it remains possible that the SM-like Higgs boson discovered at the LHC is in fact a SUSY Higgs.

The Minimal Supersymmetric Standard Model (MSSM) [4], requires at least two complex Higgs doublets. In the Next-to-Minimal SUSY model (NMSSM) [5] another complex singlet superfield is added to the Higgs sector. The coupling of the singlet field to the MSSM Higgs doublets allows for a dynamical solution of the μ problem [6] when the neutral component of the singlet field acquires its vacuum expectation value (VEV). The totality of ten degrees of freedom of the Higgs doublet and singlet fields leads to seven physical Higgs bosons after electroweak symmetry breaking. In the CP-conserving NMSSM these are three CP-even and two CP-odd neutral Higgs bosons plus two charged ones, whereas in the CP-violating case all Higgs bosons mix and do not carry a definite CP quantum number any more. Besides the direct detection of more Higgs states, an extended Higgs sector can manifest itself in modified Higgs couplings of the SM-like Higgs boson. These arise from the mixture with other Higgs states or from new physics effects induced through radiative corrections to the Higgs couplings and/or in the loop mediated Higgs interactions with the photons and gluons. Furthermore, Higgs decays into other lighter non-SM particles can be realized leading to modified branching ratios, including also the possibility of invisible decays.

CP violation is one of the three Sakharov conditions [7] for baryogenesis, leading to matter-antimatter asymmetry in the universe. In the SM the only source of CP violation is given by the Cabibbo-Kobayashi-Maskawa (CKM) matrix [8, 9]. While the SM provides the necessary ingredients for all Sakharov conditions, CP violation based on the CKM matrix is too small to explain quantitatively the observed asymmetry.[1] This motivates studying BSM theories which include additional sources of CP violation. SUSY contains many new sources of CP violation. In the MSSM CP violation in the Higgs sector itself cannot occur at tree level and is radiatively induced. In the NMSSM Higgs sector, however, CP violation can already show up at tree level through NMSSM specific complex couplings which induce CP-violating doublet-singlet mixing.

In this paper we shall be concerned with the CP-violating NMSSM, including CP-violating effects in the phenomenology of the 125 GeV Higgs boson as well as other effects in the Higgs sector as follows. For example, in the CP-violating NMSSM, a non-zero CP-odd admixture in the couplings of the dominantly CP-even non-SM-like light Higgs boson may weaken its couplings to the weak gauge bosons to such an extent that it escapes the LEP limits [10]. Additionally, CP violation in the Higgs couplings can allow for decays of Higgs bosons into Higgs and gauge bosons or a pair of lighter Higgs bosons in combinations that otherwise would be forbidden. These could then constitute additional discovery channels for some of the Higgs states. In general CP mixing alters the Higgs couplings and hence the production and decay rates with effects on the discovery

[1] Besides the fact, that the 125 GeV Higgs boson is too heavy to allow for the strong first order phase transition in the early universe required for thermal non-equilibrium.

prospects of the additional NMSSM Higgs bosons.[2] Moreover, CP-violating phases influence the Higgs mass spectrum already at tree level in case of Higgs sector CP violation and at loop level through radiatively induced CP violation [12, 13]. Some of these effects, however, can also be explained in the CP-conserving NMSSM by choosing the parameter combinations accordingly. Additionally, without further information on the CP nature of the Higgs bosons from other observables, genuine CP-violating Higgs decays to gauge boson plus Higgs or Higgs-to-Higgs decays cannot be identified unless all of these decay channels are observed. Since the absolute size of CP violation is stringently constrained by experiment, the identification of CP-violating Higgs bosons will be a non-trivial task requiring precision measurements, high luminosities and the combination of various CP-violating observables. In particular tight constraints on the CP-violating phases arise from the non-observation of electric dipole moments (EDMs). Accordingly, we discuss in detail in the main part of the paper the role of EDMs in constraining the parameter space of the CP-violating NMSSM. By taking into account the latest experimental constraints from the Higgs data and the measurements of the EDMs, we investigate the size of the EDMs as a function of the CP-violating phases. This allows for conclusions on the overall allowed size of CP violation in the NMSSM in view of the newest experimental results. Subsequently, we investigate how CP violation can be identified by combining Higgs-to-Higgs decays and Higgs decays to gauge boson plus Higgs. This is complemented by the discussion of measuring CP violation in fermionic Higgs decays.

The investigation of the CP-violating NMSSM Higgs sector considered here takes into account higher order corrections both to the parameters and the observables. Radiative corrections to the Higgs boson masses are crucial to lift the SM–like Higgs boson mass to the observed value of 125 GeV. The connection of the Higgs self-couplings and masses through the Higgs potential requires the inclusion of higher order corrections also in the Higgs self-interactions to consistently describe Higgs-to-Higgs decays, which can become relevant for spectra with light Higgs bosons and/or sizeable values of the singlet coupling λ [14–24]. In the Higgs boson decays into SM particles and coloured SUSY particles in particular QCD corrections play an important role and have to be included. Also electroweak corrections can become important. They cannot be adapted from the SM or MSSM, however, but require an explicit calculation, as has been done so far in the NMSSM only for the Higgs boson decays into squarks [25].

It is worth recalling the status of higher order corrections to the NMSSM Higgs boson masses. In the CP-conserving NMSSM the one-loop mass corrections are available [26–35], as well as two-loop results of $\mathrm{O}(\alpha_t\alpha_s + \alpha_b\alpha_s)$ in the approximation of zero external momentum [33]. First corrections beyond order $\mathrm{O}(\alpha_t\alpha_s + \alpha_b\alpha_s)$ have been provided in [36]. The one-loop corrections to the Higgs masses of the CP-violating NMSSM have been calculated by [12, 37–41] and the logarithmically enhanced two-loop effects have been given in [42]. The two-loop corrections to the Higgs boson masses of the CP-violating NMSSM in the Feynman diagrammatic approach with vanishing external momentum at $\mathrm{O}(\alpha_t\alpha_s)$ have been computed in [13]. The one-loop corrections to the trilinear Higgs self-couplings for the CP-conserving NMSSM [15] are available and have recently been extended to include the two-loop corrections at order $\mathcal{O}(\alpha_t\alpha_s)$ in the approximation of vanishing external momentum in the CP-violating case [43]. Several public codes are on the market for the computation of the NMSSM mass spectrum for a given parameter set. These are the stand-alone codes `NMSSMTools` [44–46], `SOFTSUSY` [47, 48] and `NMSSMCALC` [49, 50], and the NMSSM implementations of the programs `FlexibleSUSY` [51, 52] and `SPheno` [53, 54] which are

[2] For a recent discussion on two Higgs bosons near 125 GeV in the complex NMSSM, see [11].

based on SARAH [36, 55–58].[3] An extension of the program package NMSSMTools to include also the CP-violating NMSSM has recently been announced in [60].

For the phenomenological analysis in this paper we have implemented the EDMs in the Fortran package NMSSMCALC. It computes for the CP-conserving and CP-violating case the two-loop NMSSM Higgs boson masses at $\mathcal{O}(\alpha_t\alpha_s)$ and the Higgs boson widths and branching ratios including the dominant higher order corrections.[4]

The layout of the paper is as follows. In Section 2 we introduce the CP-violating NMSSM Lagrangian and set our notation. Section 3 briefly recapitulates the computation of the SUSY contributions to the EDMs. In Section 4 we discuss in detail the EDMs induced by various CP-violating phases present in the NMSSM. In subsection 4.1 this investigation is performed in the subspace of the Natural NMSSM that features a rather light Higgs spectrum with good discovery prospects for all Higgs bosons of the NMSSM. In subsection 4.2, we extend the investigation to an enlarged NMSSM parameter range. Section 5 is devoted to the prospects for measuring CP violation in the Higgs couplings involving Z bosons through the combination of signal rates, subsection 5.1, and in the Higgs couplings to fermions, subsection 5.2. Section 6 summarizes and concludes the paper.

2 The Lagrangian of the CP-violating NMSSM

We work in the framework of the CP-violating NMSSM with a scale-invariant superpotential and a discrete $\mathbb{Z}^3$ symmetry. The Higgs potential is obtained from the superpotential, the soft SUSY breaking Lagrangian and the D-term contributions. The NMSSM superpotential in terms of the two Higgs doublet superfields $\hat{H}_d$ and $\hat{H}_u$, the singlet superfield $\hat{S}$, the quark and lepton superfields and their charged conjugates, with the superscript c, $\hat{Q}, \hat{U}^c, \hat{D}^c, \hat{L}, \hat{E}^c$, is given by

$$W_{NMSSM} = \epsilon_{ij}[y_e \hat{H}_d^i \hat{L}^j \hat{E}^c + y_d \hat{H}_d^i \hat{Q}^j \hat{D}^c - y_u \hat{H}_u^i \hat{Q}^j \hat{U}^c] - \epsilon_{ij}\lambda \hat{S} \hat{H}_d^i \hat{H}_u^j + \frac{1}{3}\kappa \hat{S}^3 \,. \tag{2.1}$$

The $i, j = 1, 2$ are the indices of the $SU(2)_L$ fundamental representation, and ϵ_{ij} is the totally antisymmetric tensor with $\epsilon_{12} = \epsilon^{12} = 1$, where we adopt the convention to sum over equal indices. Colour and generation indices have been suppressed. As we neglect generation mixing, the Yukawa couplings y_e, y_d and y_u are diagonal, and complex phases can be reabsorbed by redefining the quark fields without effect on the physical meaning [9]. The dimensionless parameters λ and κ are complex in case of CP violation.

The soft SUSY breaking Lagrangian in terms of the scalar component fields H_u, H_d and S reads

$$\begin{aligned}
\mathcal{L}_{\text{soft, NMSSM}} = &- m_{H_d}^2 H_d^\dagger H_d - m_{H_u}^2 H_u^\dagger H_u - m_{\tilde{Q}}^2 \tilde{Q}^\dagger \tilde{Q} - m_{\tilde{L}}^2 \tilde{L}^\dagger \tilde{L} - m_{\tilde{u}_R}^2 \tilde{u}_R^* \tilde{u}_R - m_{\tilde{d}_R}^2 \tilde{d}_R^* \tilde{d}_R \\
&- m_{\tilde{e}_R}^2 \tilde{e}_R^* \tilde{e}_R - (\epsilon_{ij}[y_e A_e H_d^i \tilde{L}^j \tilde{e}_R^* + y_d A_d H_d^i \tilde{Q}^j \tilde{d}_R^* - y_u A_u H_u^i \tilde{Q}^j \tilde{u}_R^*] + \text{h.c.}) \\
&- \frac{1}{2}(M_1 \tilde{B}\tilde{B} + M_2 \tilde{W}_i \tilde{W}_i + M_3 \tilde{G}\tilde{G} + \text{h.c.}) \\
&- m_S^2 |S|^2 + (\epsilon_{ij}\lambda A_\lambda S H_d^i H_u^j - \frac{1}{3}\kappa A_\kappa S^3 + \text{h.c.}) \,,
\end{aligned} \tag{2.2}$$

[3] For a comparison of the codes, see [59].

[4] The program package NMSSMCALC including the computation of the EDMs is made publicly available and can be downloaded from the url: http://www.itp.kit.edu/∼maggie/NMSSMCALC/.

where a sum over all three quark and lepton generations is implicit. The $\tilde{Q}$ and $\tilde{L}$ denote the complex scalar components of the corresponding quark and lepton superfields and, *e.g.* for the first generation are $\tilde{Q} = (\tilde{u}_L, \tilde{d}_L)^T$ and $\tilde{L} = (\tilde{\nu}_L, \tilde{e}_L)^T$. In the CP-violating NMSSM the soft SUSY breaking trilinear couplings A_x ($x = \lambda, \kappa, d, u, e$) and the gaugino mass parameters M_k ($k = 1, 2, 3$) of the bino, wino and gluino fields $\tilde{B}, \tilde{W}_i$ ($i = 1, 2, 3$) and $\tilde{G}$, are complex. Exploiting the R-symmetry either M_1 or M_2 can be chosen to be real. On the other hand the soft SUSY breaking mass parameters of the scalar fields, m_X^2 ($X = S, H_d, H_u, \tilde{Q}, \tilde{u}_R, \tilde{d}_R, \tilde{L}, \tilde{e}_R$) are real.

The Higgs potential finally is obtained as

$$\begin{aligned} V_H &= (|\lambda S|^2 + m_{H_d}^2) H_d^\dagger H_d + (|\lambda S|^2 + m_{H_u}^2) H_u^\dagger H_u + m_S^2 |S|^2 \\ &\quad + \frac{1}{8}(g_2^2 + g_1^2)(H_d^\dagger H_d - H_u^\dagger H_u)^2 + \frac{1}{2} g_2^2 |H_d^\dagger H_u|^2 \\ &\quad + |-\epsilon^{ij} \lambda H_{d,i} H_{u,j} + \kappa S^2|^2 + \big[-\epsilon^{ij} \lambda A_\lambda S H_{d,i} H_{u,j} + \frac{1}{3} \kappa A_\kappa S^3 + \text{h.c.} \big] \,, \end{aligned} \tag{2.3}$$

with g_1 and g_2 denoting the $U(1)_Y$ and $SU(2)_L$ gauge couplings, respectively. Expanding the two Higgs doublets and the singlet field about their VEVs, v_d, v_u and v_s, two more CP-violating phase, φ_u and φ_s, are introduced,

$$H_d = \begin{pmatrix} \frac{1}{\sqrt{2}}(v_d + h_d + i a_d) \\ h_d^- \end{pmatrix}, \quad H_u = e^{i\varphi_u} \begin{pmatrix} h_u^+ \\ \frac{1}{\sqrt{2}}(v_u + h_u + i a_u) \end{pmatrix}, \quad S = \frac{e^{i\varphi_s}}{\sqrt{2}}(v_s + h_s + i a_s) \,. \tag{2.4}$$

The VEVs v_u and v_d are related to $v \approx 246$ GeV through $v^2 = v_d^2 + v_u^2$ and their ratio is parametrized by $\tan\beta = v_u/v_d$. The phase φ_u affects the top quark mass. We absorb this phase into the left-handed and right-handed top fields through

$$t_L \to e^{-i\varphi_u/2}\, t_L \quad \text{and} \quad t_R \to e^{i\varphi_u/2}\, t_R \,, \tag{2.5}$$

so that the top Yukawa coupling is kept real. This alters all couplings with one top quark. Replacing Eq. (2.4) in Eq. (2.3) yields the Higgs potential

$$\begin{aligned} V_H &= V_H^{\text{const}} + t_{h_d} h_d + t_{h_u} h_u + t_{h_s} h_s + t_{a_d} a_d + t_{a_u} a_u + t_{a_s} a_s \\ &\quad + \frac{1}{2} \phi^{0,T} \mathcal{M}_{\phi\phi}\, \phi^0 + \phi^{c,\dagger} \mathcal{M}_{h^+h^-}\, \phi^c + V_H^{\phi^3,\phi^4} \,, \end{aligned} \tag{2.6}$$

with $\phi^0 \equiv (h_d, h_u, h_s, a_d, a_u, a_s)^T$ and $\phi^c \equiv ((h_d^-)^*, h_u^+)^T$. The tadpole coefficients are denoted by t_ϕ ($\phi = h_d, h_u, h_s, a_d, a_u, a_s$), $\mathcal{M}_{\phi\phi}$ is the 6×6 mass matrix for the neutral Higgs bosons and $M_{h^+h^-}$ the 2×2 mass matrix for the charged Higgs states. Constant terms are summarized in V_H^{const} and the trilinear and quartic interactions in $V_H^{\phi^3,\phi^4}$. A few remarks on the tadpoles and mass matrices are in order, without repeating their explicit expressions here, which can be found in Ref. [12]. The tadpole coefficients vanish at tree level due to the minimization conditions of the Higgs potential. Rewriting the complex parameters $\lambda, \kappa, A_\lambda$ and A_κ as

$$\lambda = |\lambda| e^{i\varphi_\lambda} \,,\ \kappa = |\kappa| e^{i\varphi_\kappa} \,,\ A_\lambda = |A_\lambda| e^{i\varphi_{A_\lambda}} \quad \text{and} \quad A_\kappa = |A_\kappa| e^{i\varphi_{A_\kappa}} \,, \tag{2.7}$$

three phase combinations appear at tree level in the tadpoles and the mass matrices,

$$\varphi_x = \varphi_{A_\lambda} + \varphi_1 \,, \tag{2.8}$$

$$\varphi_y = \varphi_2 - \varphi_1 \,, \tag{2.9}$$

$$\varphi_z = \varphi_{A_\kappa} + \varphi_2 \,, \tag{2.10}$$

where we have introduced

$$\varphi_1 = \varphi_\lambda + \varphi_s + \varphi_u \,, \tag{2.11}$$
$$\varphi_2 = \varphi_\kappa + 3\varphi_s \,. \tag{2.12}$$

Two of the three combinations Eqs. (2.8)-(2.10) can be eliminated at lowest order by applying the minimization conditions $t_{a_d} = t_{a_s} = 0$. We express φ_x and φ_z in terms of φ_y. All mass matrix elements mixing the CP-even and CP-odd interaction states, $\mathcal{M}_{h_i a_j}$, are then proportional to $\sin\varphi_y$. At tree level, this is the only CP-violating phase in the Higgs sector. The rotation from the interaction to the mass eigenstates h_i $(i = 1, ..., 5)$ is performed by applying two consecutive rotations. The first rotation with matrix $\mathcal{R}^G$ separates the would-be Goldstone bosons. The second one with the matrix $\mathcal{R}$ performs the rotation to the mass eigenstates, *i.e.*

$$\begin{aligned} (h_d, h_u, h_s, a, a_s, G)^T &= \mathcal{R}^G \, (h_d, h_u, h_s, a_d, a_u, a_s)^T \,, \\ (h_1, h_2, h_3, h_4, h_5, G)^T &= \mathcal{R} \, (h_d, h_u, h_s, a, a_s, G)^T \,, \end{aligned} \tag{2.13}$$

with the diagonal mass matrix

$$\mathrm{diag}(m^2_{h_1}, m^2_{h_2}, m^2_{h_3}, m^2_{h_4}, m^2_{h_5}, 0) = \mathcal{R}\mathcal{M}_{hh}\mathcal{R}^T \,, \quad \mathcal{M}_{hh} = \mathcal{R}^G \mathcal{M}_{\phi\phi} (\mathcal{R}^G)^T . \tag{2.14}$$

The mass eigenstates h_i are ordered by ascending mass, where the lightest mass is given by m_{h_1}.

The tree-level Higgs potential can be parametrized by the following set of independent parameters

$$t_{h_d}, t_{h_u}, t_{h_s}, t_{a_d}, t_{a_s}, M^2_{H^\pm}, v, \sin\theta_W, e, \tan\beta, |\lambda|, v_s, |\kappa|, \mathrm{Re}A_\kappa, \sin\varphi_y \,. \tag{2.15}$$

We have chosen to use v and $\sin\theta_W$, where θ_W denotes the weak mixing angle, instead of M_W and M_Z. This is more convenient in view of the inclusion of the two-loop corrections to the Higgs boson masses in the gaugeless limit.[5] Furthermore, in accordance with the SUSY Les Houches Accord (SLHA) [61, 62] the real part of A_κ is used as input parameter. The imaginary part is eliminated by the tadpole conditions. This distinction is not necessary for λ and κ, as both the real and imaginary parts are given in the SLHA convention and can be related to the respective absolute values and phases. Note finally, that the effective higgsino mixing parameter is given by

$$\mu_{\text{eff}} = \frac{|\lambda| v_s e^{i(\varphi_s + \varphi_\lambda)}}{\sqrt{2}} \,. \tag{2.16}$$

At higher order in the Higgs mass corrections (and self-couplings) the CP-violating phases entering the Higgs sector at tree level are not related any more. The phases φ_1 and φ_2 appear independently in the neutralino sector, while the chargino and up-type squark sector depend on the phase φ_1. We therefore have two independent CP-violating phases that appear, if we choose to determine the phases φ_{A_κ} and φ_{A_λ} from the tadpole conditions. Of course non-vanishing φ_1 or φ_2 will automatically imply non-vanishing φ_{A_λ} and φ_{A_κ}. However, since we consider the latter two as derived quantities, which are fixed via the tadpole conditions, we will not mention them explicitly in the following discussion. The higher order corrections introduce further complex phases stemming from the complex soft SUSY breaking trilinear couplings and gaugino mass parameters, that enter the couplings and SUSY particle masses involved in the loop corrections.

[5] See [13] for details.

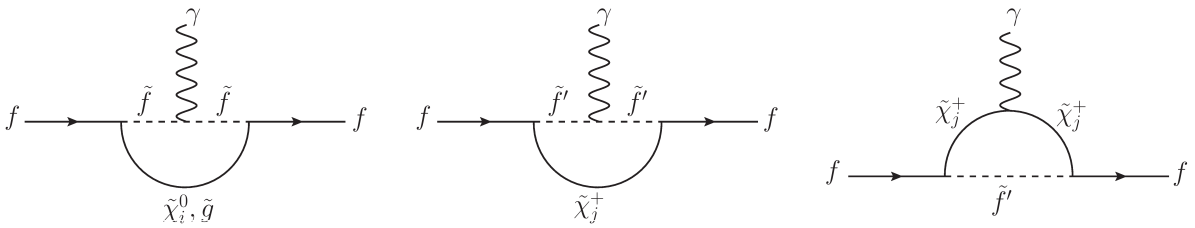

Figure 1: Generic one-loop diagrams contributing to the EDMs of the electron and light quarks ($f = e, u, d, s$).

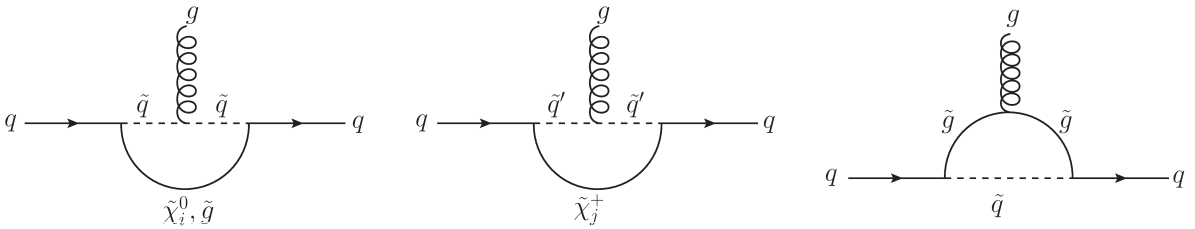

Figure 2: Generic one-loop diagrams contributing to the CEDMs of the light quarks ($q = u, d, s$).

3 Electric Dipole Moments

CP violation would manifest itself in the generation of EDMs. The non-observation of any EDMs so far poses stringent constraints on CP-violating phases. These have to be taken into account, when discussing possible CP-violating effects in the Higgs sector. The constraints may become weaker in case of accidental cancellations of the various contributions to the EDMs, even for lighter SUSY particles with masses below $\mathcal{O}(1\text{ TeV})$ [63, 64]. In our analysis we take into account all relevant CP-induced contributions to the observable EDMs. In particular we consider the compatibility with the experimental upper bounds on the EDMs, which are

$$\begin{aligned}
&\text{Electron EDM [65]} &&: \sim 1 \cdot 10^{-28} e\,\text{cm} \\
&\text{Thallium EDM [66]} &&: \sim 9 \cdot 10^{-25} e\,\text{cm} \\
&\text{Neutron EDM [67]} &&: \sim 3 \cdot 10^{-26} e\,\text{cm} \\
&\text{Mercury EDM [68]} &&: \sim 3.1 \cdot 10^{-29} e\,\text{cm}\,,
\end{aligned} \tag{3.17}$$

where the electron EDM is estimated from the thorium monoxide experiment. These observable EDMs receive form factor contributions from the electric dipole moment, the chromo-electric dipole moment (CEDM), the two-loop Weinberg three-gluon operator and the Higgs-exchange four-fermion operators. All of these contain contributions that are generated by CP-violating Higgs mixing at tree level. In the EDM and the CEDM we consider one- and two-loop contributions. The two-loop contributions stemming from CP violation in the Higgs sector at tree level, which is specific to the NMSSM, can become important when the CP phases of the MSSM parameters are set to zero [69]. Such a configuration can be achieved by choosing $\varphi_2 \neq 0$, while keeping $\varphi_1 = 0$. Therefore we will refer to φ_2 as the NMSSM-specific phase in the following. The one-loop EDMs of the electron and the light quarks u, d, s are induced by chargino, $\tilde{\chi}_j^\pm$ ($j = 1, 2$), and neutralino, $\tilde{\chi}_i^0$ ($i = 1, ..., 5$), exchange diagrams, *cf.* Fig. 1. For the quarks also gluino, $\tilde{g}$, exchange diagrams contribute. The light quarks furthermore have CEDMs which are also generated by chargino, neutralino and gluino loops as shown in Fig. 2. The one-loop EDMs

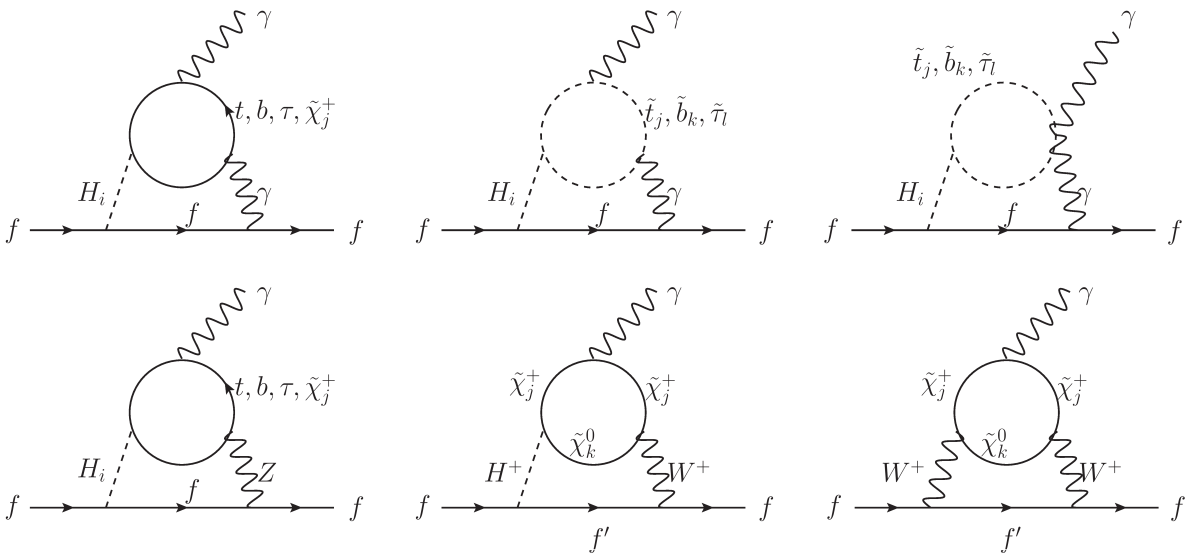

Figure 3: Generic two-loop Barr-Zee type diagrams contributing to the EDMs of the electron and light quarks ($f = e, u, d, s$). Upper: γH, and lower from left to right: ZH, WH and WW.

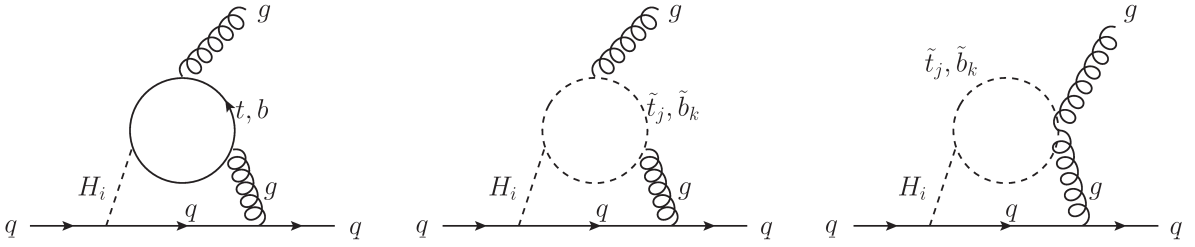

Figure 4: Generic two-loop Barr-Zee type diagrams contributing to the CEDMs of the light quarks ($q = u, d, s$).

have been computed before and the formulae can be found in [64, 69]. At two-loop level the Higgs mediated Barr-Zee type diagrams contribute significantly to the EDMs. They are mediated by neutral Higgs couplings to two photons, $\gamma\gamma H_i^0$ [64], the charged Higgs coupling to the charged W boson and a photon, $\gamma H^\pm W^\mp$, the $\gamma W^\pm W^\mp$coupling [70], and the couplings between a neutral Higgs boson, a photon and a Z boson, $\gamma H_i^0 Z$ [71]. We will denote these contributions in the following as γH, WH, WW and ZH, respectively. The diagrams are displayed in Fig. 3. Additionally, CEDMs of the light quarks u, d and s are generated by two-loop Higgs-mediated Barr-Zee graphs [64, 69], *cf.* Fig. 4. For the Weinberg operator we take into account the contributions from the Higgs-mediated two-loop diagrams [72] and additionally the contribution from the quark-squark-gluino exchange contribution [73]. The coefficients of the four-fermion operators, finally, are generated from the t-channel exchanges of the CP-violating neutral Higgs bosons [64].

We briefly describe how the observable EDMs are obtained from the various contributions introduced above. For explicit formulae and more details we refer the reader to [64, 69] and references therein. The Thallium EDM receives contributions from the electron EDM and additionally from the CP-odd electron-nucleon interaction [74, 75]. For the neutron EDM three different hadronic approaches are considered. These are the Chiral Quark Model (CQM), the

Parton Quark Model (PQM) and the QCD sum rule technique. In the non-relativistic CQM the quark EDMs are estimated via naive dimensional analysis [76]. The PQM uses low-energy data related to the constituent-quark contribution to the proton spin combined with isospin symmetry [77]. In the third approach finally QCD sum rule techniques [78–80] are applied to determine the EDM. Depending on the approach, the neutron EDM is composed of the contributions from the EDMs and CEDMs of the light quarks, the Weinberg operator and the CP-odd four-fermion operators, see [64] for details. By using QCD sum rules [78, 80] the Mercury EDM is estimated from the EDMs induced by the Schiff moment[6], the electron EDM, the contribution due to the CP-odd electron-nucleon interaction and the contributions from the couplings of electron-nucleon interactions. Details are given in [69].

4 EDM constraints

In this section we investigate the influence of the various CP-violating phases on the EDMs and the resulting constraints on possible CP-violating scenarios. We will present results for the phases φ_1, φ_2 and the phase φ_{A_t}, which arises from the top/stop sector, and the phases φ_{M_i} of the gaugino mass parameters M_i $(i = 1, 2, 3)$. The EDMs also depend on the phases φ_{A_j} of the soft SUSY breaking trilinear couplings A_j $(j = b, u, c, d, s)$. The influence of the phases φ_{A_j} of the sbottom and the first and second generation squark sector is by far subleading compared to the effects of the other phases. The reason is that the trilinear couplings and hence their phases come in combination with the quark masses, which are small in this case.

In order to find viable parameter points we perform a scan in the NMSSM parameter space and keep only those points that are in accordance with the LHC Higgs data. That this is the case has been checked with the help of the programs `HiggsBounds` [82–84] and `HiggsSignals` [85]. For the computation of the Higgs boson masses, the effective couplings, the decay widths and branching ratios of the SM and NMSSM Higgs bosons, that are needed as inputs for `HiggsBounds` and `HiggsSignals`, the Fortran code `NMSSMCALC` [49, 50] has been used. Besides the masses at two-loop level, it provides the SM and NMSSM decay widths and branching ratios including the state-of-the-art higher order corrections. We demanded that the valid scenarios feature a Higgs boson with mass around 125 GeV. With `HiggsBounds` we have checked whether or not the Higgs spectrum is excluded at the 95% confidence level (CL) with respect to the LEP, Tevatron and LHC measurements. The package `HiggsSignals` tests for the compatibility of the SM-like Higgs boson with the Higgs observation data. We required the p-value, that is given out, to be at least 0.05, corresponding to a non-exclusion at 95% CL.

4.1 Natural NMSSM

We performed a parameter scan in the subspace of the Natural NMSSM as defined in [21]. It features a rather light overall Higgs mass spectrum and gives good discovery prospects for all NMSSM Higgs scalars. It is characterized by

$$0.6 \leq |\lambda| \leq 0.7\,,\ |\kappa| \leq 0.3\,,\ 1.5 \leq \tan\beta \leq 2.5\,,\ 100\ \text{GeV} \leq |\mu_{\text{eff}}| \leq 185\ \text{GeV}\,. \tag{4.18}$$

The small κ values lead to an approximate Peccei-Quinn symmetry. Note, that in this parameter region the second lightest of the Higgs bosons that are dominantly CP-even, is SM-like[7]. The

[6] For the Schiff moment several approximations exist [81].

[7] The Higgs boson with mass close to 125 GeV is forced to be mostly CP-even due to the requirement to be compatible with the LHC Higgs data.

soft SUSY breaking trilinear NMSSM couplings are varied in the interval

$$|A_\lambda| \leq 2 \text{ TeV} \qquad \text{and} \qquad |A_\kappa| \leq 2 \text{ TeV} \,. \tag{4.19}$$

The remaining soft SUSY breaking trilinear couplings and masses have been chosen as

$$|A_U|, |A_D|, |A_L| \leq 2 \text{ TeV} \qquad \text{with} \qquad U \equiv u, c, t, \;, D \equiv d, s, b \,, L = e, \mu, \tau, \tag{4.20}$$

$$M_{\tilde{u}_R, \tilde{c}_R} = M_{\tilde{d}_R, \tilde{s}_R} = M_{\tilde{Q}_{1,2}} = M_{\tilde{e}_R, \tilde{\mu}_R} = M_{\tilde{L}_{1,2}} = 3 \text{ TeV} \,, \tag{4.21}$$

$$600 \text{ GeV} \leq M_{\tilde{t}_R} = M_{\tilde{Q}_3} \leq 3 \text{ TeV} \,, \; 600 \text{ GeV} \leq M_{\tilde{\tau}_R} = M_{\tilde{L}_3} \leq 3 \text{ TeV} \,, \; M_{\tilde{b}_R} = 3 \text{ TeV} \,, \tag{4.22}$$

$$100 \text{ GeV} \leq |M_1| \leq 1 \text{ TeV} \,, \; 200 \text{ GeV} \leq |M_2| \leq 1 \text{ TeV} \,, \; 1.3 \text{ TeV} \leq |M_3| \leq 3 \text{ TeV} \,. \tag{4.23}$$

All scenarios have been checked for compatibility with the lower bound on the charged Higgs mass [86] and respect the exclusion limits on the SUSY particle masses [87–89]. Note also, that the signs of the gaugino masses M_1 and M_2 have only a marginal effect on the features of the NMSSM Higgs sector. The NMSSM-specific input parameters $\lambda, \kappa, A_\lambda$ and A_κ as well as all other soft SUSY breaking masses and trilinear couplings, according to the SLHA format, are understood as $\overline{\text{DR}}$ parameters taken at the SUSY scale $M_S = \sqrt{M_{\tilde{t}_R} M_{\tilde{Q}_3}}$. In `NMSSMCALC` also $\tan\beta$ is assumed to be given at the SUSY scale.

Variation of φ_2: For the scenarios of our scan that are compatible with all above described constraints we computed the various EDMs and checked for their compatibility with the experimental values. The results are shown in Fig. 5 for the electron, the Thallium, the neutron and the Mercury EDM. In these plots we have only varied the NMSSM specific phase φ_2. All other complex phases have been set to zero. We hence investigate here solely tree-level CP violation, as it can occur in the NMSSM. As the phase φ_2 only appears in the NMSSM we call this in the following *NMSSM-type CP violation*. For each EDM, the absolute values of the computed EDMs in the valid scenarios are shown, normalized to the respective experimental upper bound, as given in Eq. (3.17). All points above 1 are hence in conflict with the EDM data. For the neutron EDM results are given for two different hadronic approaches, the chiral quark model and the one applying QCD sum rule techniques, Fig. 5 (middle row).[8] In the Mercury EDM, Fig. 5 (lower row), we have taken into account the uncertainties in the calculation of the contribution from the Schiff moment by showing results for two of the four values given in the literature, $d_{\text{Hg}}^{\text{I,II,III,IV}}[S]$ [69,81]. The superscripts in d_{Hg} indicate which value has been applied. As can be inferred from the plots the most stringent constraints arise from the electron EDM, Fig. 5 (upper left). The constraints from the Thallium EDM, Fig. 5 (upper right), which mostly depends on the electron EDM dE_e, are not as stringent. The results for the neutron EDM based on the CQM and the QCD sum rule technique differ by about a factor 2-3 in accordance with previous results in the literature [60, 69]. The pictures for the Mercury EDM based on $\text{d}_{\text{Hg}}^{\text{I}}$ and $\text{d}_{\text{Hg}}^{\text{IV}}$ are almost the same and similar to the ones based on $\text{d}_{\text{Hg}}^{\text{II}}$ and $\text{d}_{\text{Hg}}^{\text{III}}$, which are not shown here. The electron EDM is larger for larger values of $|\kappa\lambda|$, *i.e.* $|\kappa\lambda| > 0.1$. Note, that CP violation in the tree-level Higgs sector is induced by terms proportional to $|\kappa\lambda| \sin(\varphi_1 - \varphi_2)$ so that for larger absolute values of $|\kappa\lambda|$ the CP-violating phase plays a more important role in the EDM. The figures show, that despite the exclusion of some points by the tight electron EDM constraints, scenarios are viable that feature a large CP-violating phase, including possible maximum CP violation $\varphi_2 = \pm\pi/2$. Finally let us remark that the asymmetry in the scattering of the points

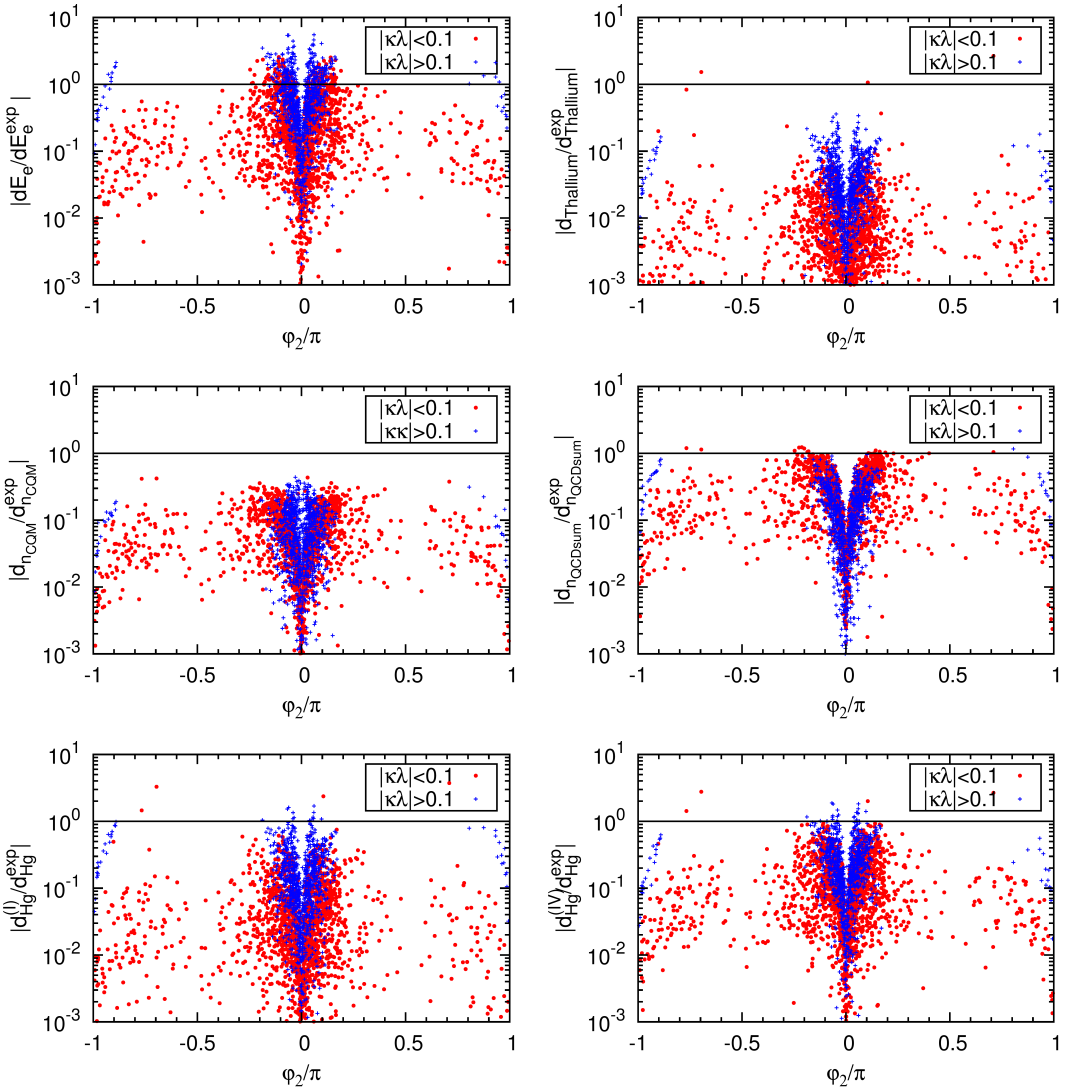

Figure 5: Absolute values of the electron (upper left), Thallium (upper right), neutron (middle) and Mercury (lower) EDMs as a function of φ_2, normalized to the respective experimental upper bound; red: $|\kappa\lambda| < 0.1$, blue: $|\kappa\lambda| > 0.1$.

at $\varphi_2 = 0$ and $\pm\pi$ is due to the fact, that our scan only extends over positive values of λ and that κ appears always in the product $\kappa\lambda$.

Investigating the various contributions in detail, we find that at one-loop level only the neutralino exchange diagrams contribute to the electron EDM. All other one-loop contributions do not depend on φ_2. The one-loop contributions turn out to be well below the exclusion bounds. The dominant part comes from the two-loop diagrams where the γH contribution is the most relevant one, but also WW is significant and comes with a different sign, see Fig. 6. The WH and ZH contributions are about an order of magnitude smaller.

The analysis of the Thallium EDM shows that the one-loop contributions are tiny. The

[8] In `NMSSMCALC` we also implemented the Parton Quark Model, but do not show explicit results here.

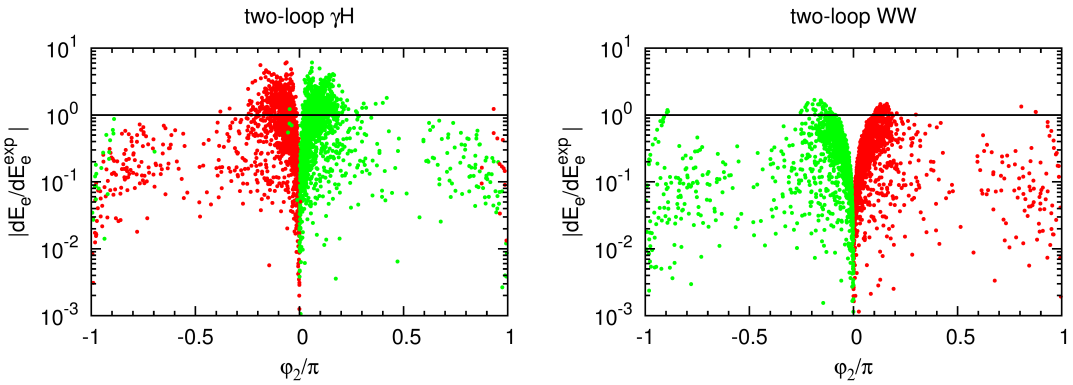

Figure 6: Absolute values of the two-loop γH (left) and WW (right) contributions to the electron EDM normalized to the experimental upper bound. Red points represent contributions with negative sign, green points those with positive sign.

two-loop and the four-fermion operator contributions are roughly of the same size and come with opposite sign, so that they partly cancel each other. Concerning the neutron EDM both in the CQM and in the QCD sum rule approximation the one-loop contributions are irrelevant and the two-loop part is dominated by the Weinberg operator contribution and the Barr-Zee type contributions to the CEDM of the quarks. In the QCD sum rule approach the latter two come with opposite signs. The four-fermion operator part that also contributes here, is small. The largest contributions to the Mercury EDM originate from the electron EDM. Also the contributions induced by the Schiff moment are of comparable order, but come with a different sign.

Variation of φ_{A_t}: We now turn to the discussion of the effects of a non-vanishing phase of the stop trilinear soft SUSY breaking coupling, φ_{A_t}. This is a phase that also appears in the MSSM and we call this in the following *MSSM-type CP violation*. Figure 7 shows the absolute values of the observable EDMs computed for the NMSSM scenarios from our scan normalized to the experimental upper bounds, now as a function of φ_{A_t}. All other possible CP-violating phases have been set to zero. As can be inferred from the figure, the most important observable EDMs induced by φ_{A_t} are the electron EDM dE_e, Fig. 7 (upper left), and the neutron EDM dn, Fig. 7 (middle row), both, however, being well below the experimental values for most of the parameter points. In the Mercury EDMs differences in the application of different Schiff moment contributions are now well visible. They are not of relevance though, as the obtained values remain below the experimental limit.

Note that a non-zero phase φ_{A_t} can induce at one-loop level only for the up-quark an EDM and a CEDM through the neutralino and gluino exchange diagrams, but solely when stops are involved, *cf.* Figs. 1 and 2. At two-loop level, besides the Weinberg operator, only the Barr-Zee type diagrams γH lead to a non-vanishing contribution, *cf.* Figs. 3 and 4. All other diagrams involve no couplings which contain φ_{A_t}. Therefore the electron and the Thallium EDM only receive two-loop γH contributions, *cf.* Fig. 3 (upper), which change sign with the phase φ_{A_t}. In the neutron EDM the two-loop contributions, which also include those from the Weinberg operator, are about one to two orders of magnitude larger than the one-loop contributions, depending on the approximation. Both come with opposite sign, *cf.* Fig. 8. The Weinberg operator provides the dominant part at two-loop level, while the EDM and CEDM contributions

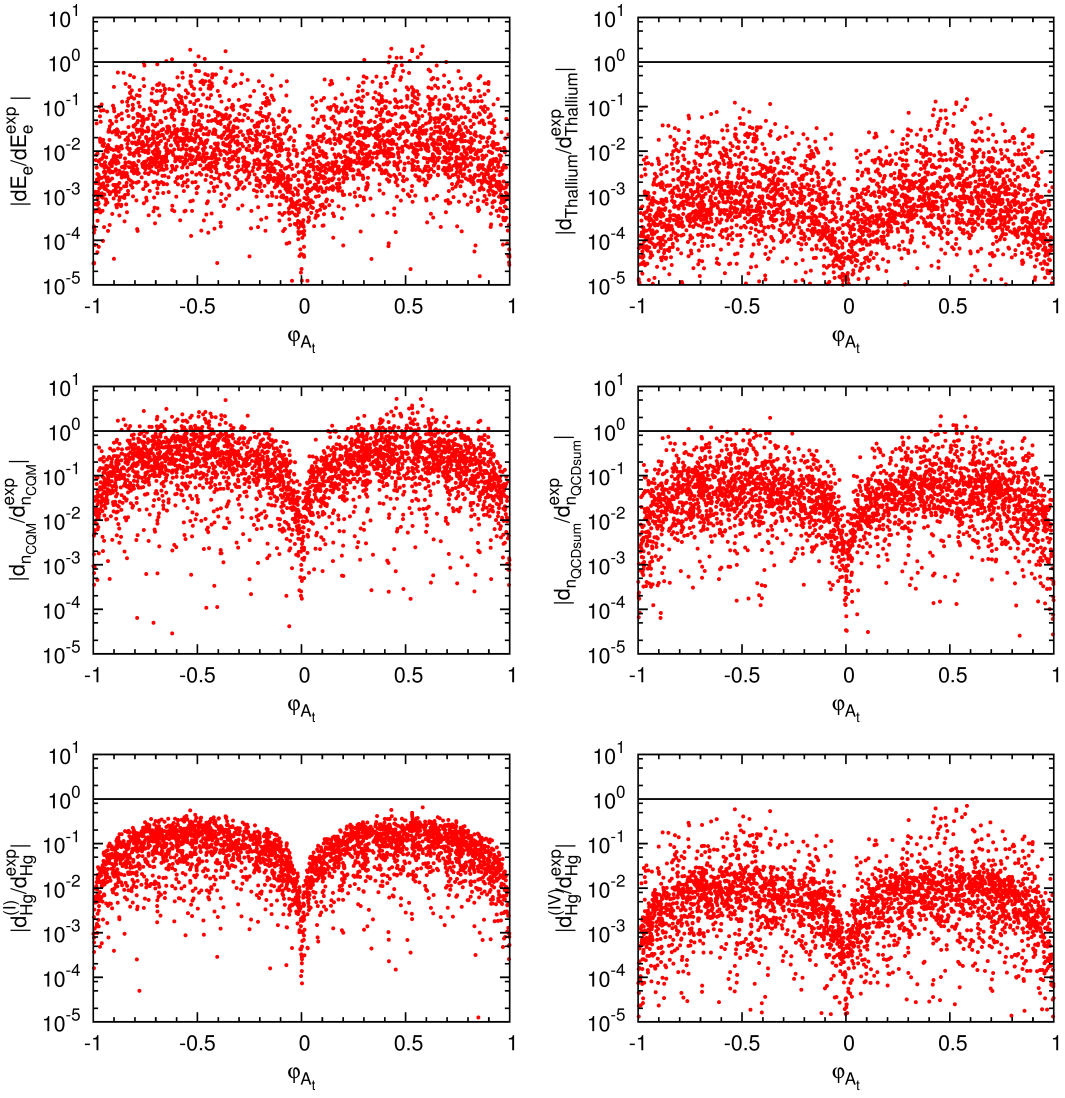

Figure 7: Same as Fig. 5, but for the variation of φ_{A_t}. All other CP-violating phases are set to zero.

to the quarks, which enter at one- and two-loop level, are of about the same size and come with opposite sign.

Variation of φ_1: A non-vanishing phase φ_1 leads to CP violation in the Higgs sector already at tree level and hence generates an *NMSSM-type CP violation*. As the phase φ_1 also enters the effective higgsino parameter $\mu_{\rm eff}$, *cf.* Eq. (2.16), it also generates CP violation in the doublet higgsino and in the sfermion sector as it occurs in the MSSM, and therefore leads to *MSSM-type CP violation*. In Fig. 9 we show the effect of a complex phase φ_1 on the values of the EDMs. All other phases have been set to zero. As can be inferred from the plots, CP violation induced by φ_1 is strongly constrained by the EDMs. In particular the induced electron EDM is by a factor up to 100 times larger than the experimental upper bound. At one-loop level the chargino contributions, that are MSSM-like, are important. The Barr-Zee type two-loop contributions are an order of magnitude larger than the ones induced by $\varphi_2 \neq 0$. In the Thallium EDM the

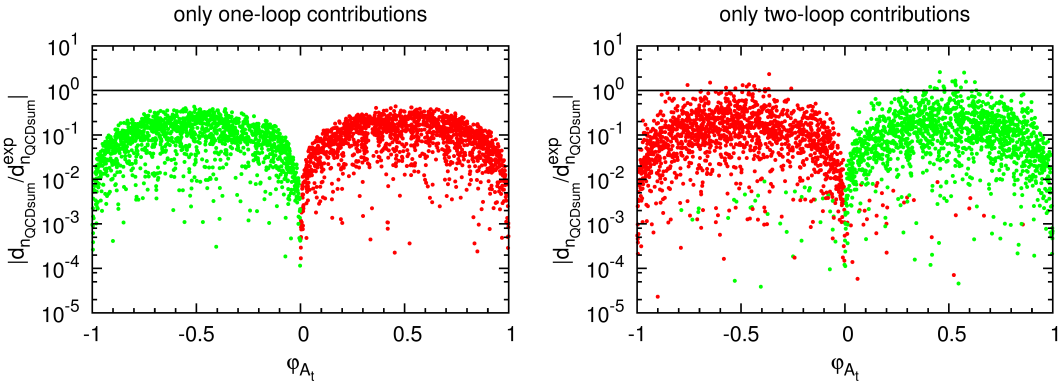

Figure 8: Absolute values of the one- (left) and two-loop contributions to the neutron EDM in the QCD sum rule approach, normalized to the measured upper bound. Red points represent contributions with negative sign, green points those with positive sign.

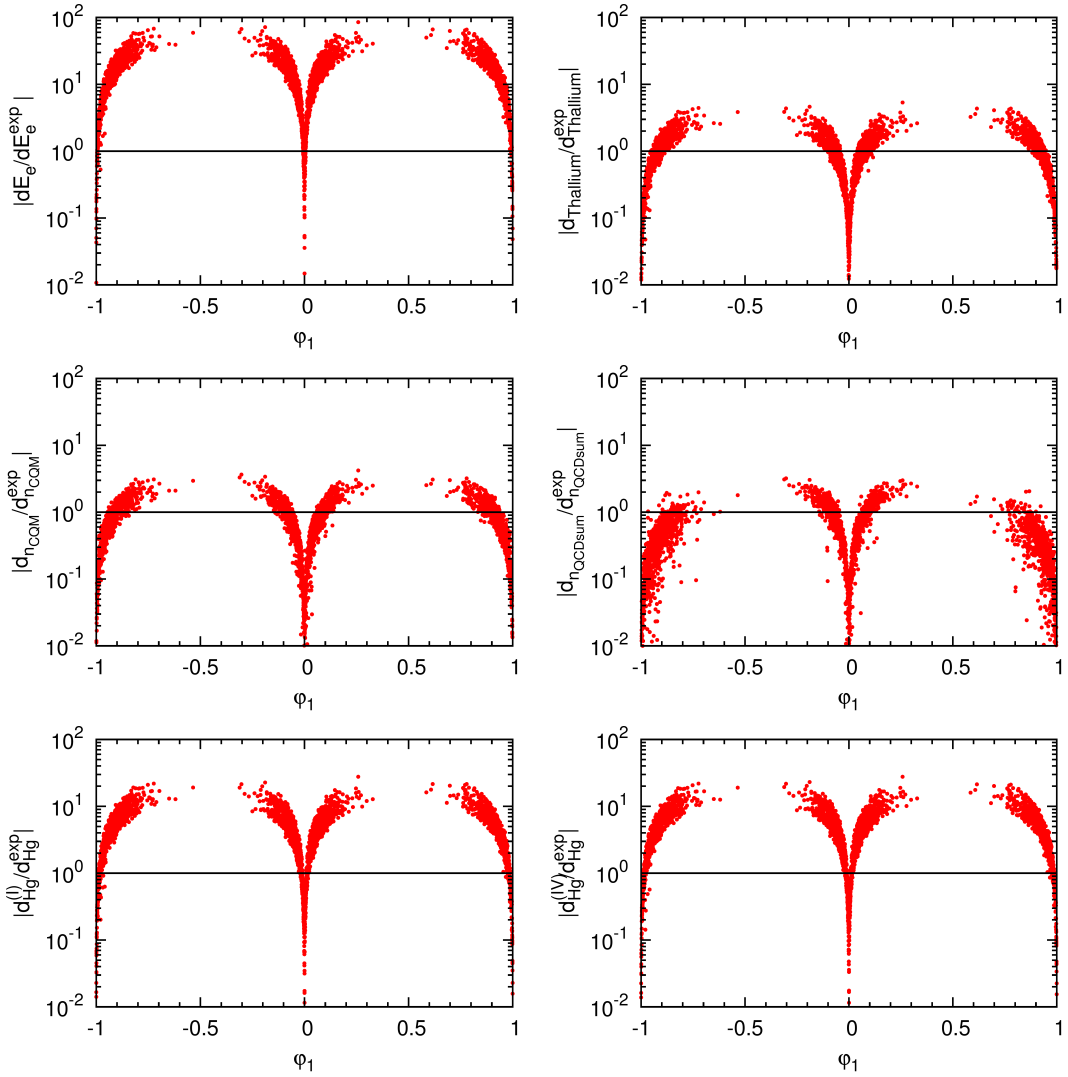

Figure 9: Absolute values of the electron (upper left), Thallium (upper right), neutron (middle) and Mercury (lower) EDMs as a function of φ_1, normalized to the respective experimental upper bound.

one- and two-loop contributions are of same size and come with the same sign. They dominate over the four-fermion operator part. For the neutron EDM the one-loop contributions dominate, while the contributions originating from the two-loop diagrams and the Weinberg operator are about one order of magnitude smaller and cancel each other partly. In the Mercury EDM, the dominant part is built up by the electron EDM.

In order to disentangle how much of the observed effect originates from NMSSM-type or, respectively, MSSM-type CP violation, we varied the phases φ_1 and φ_2 at the same time. Setting $\varphi_1 = \varphi_2$ allows to turn off tree-level CP violation in the NMSSM Higgs sector, since this yields a vanishing CP-violating phase in the tree-level Higgs sector. Hence only the CP-violating MSSM-type contributions induced by φ_1 remain. The resulting plots, which we do not show explicitly here, look strikingly similar to Fig. 9. The major difference is that in Fig. 9 there are hardly any points around the maximally CP-violating phases $\varphi_1 = \pm\pi/2$, whereas for the $\varphi_1 = \varphi_2$ variation these points exist. The gap in Fig. 9 around $\varphi_1 = \pm\pi/2$ can be attributed to the fact that we demand compatibility with the Higgs data. However, if the CP violation in the tree-level Higgs sector is too strong, *i.e.* if the CP-odd admixture of the SM-like boson becomes too large, the signals of the SM-like Higgs boson are not compatible with the experimental values any more. Regarding the EDMs we conclude that in the parameter space of the Natural NMSSM the MSSM-type CP-violating contributions induced by φ_1 dominate by far over the NMSSM-ones generated by φ_1.

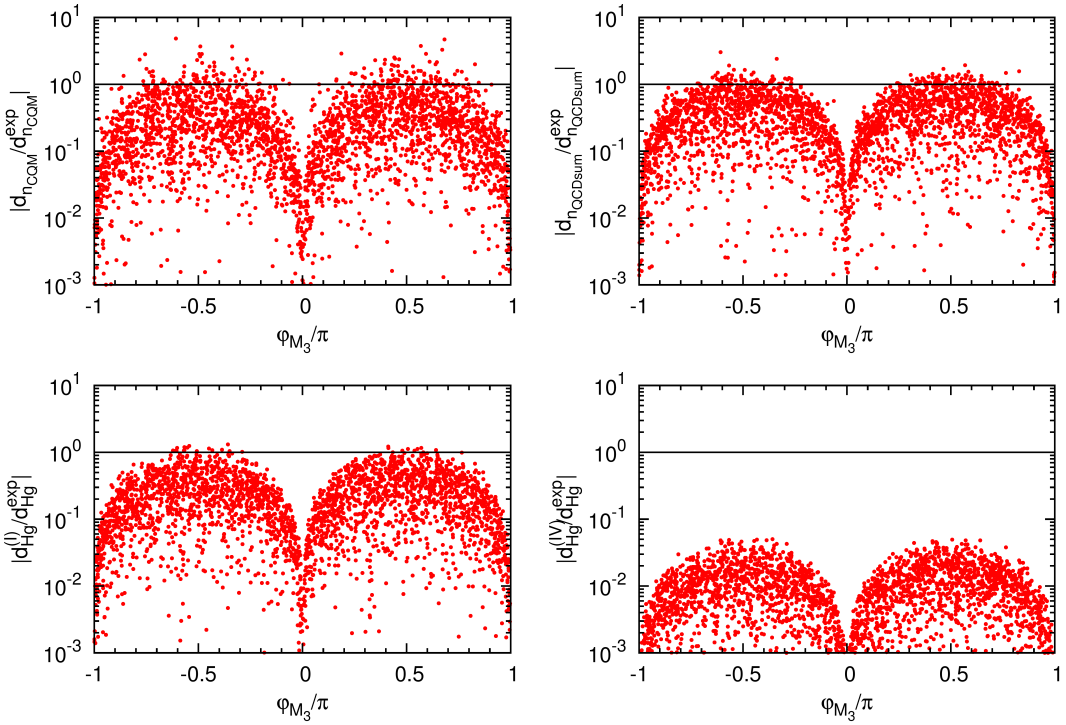

Figure 10: Absolute values of the neutron (upper) and Mercury (lower) EDMs as a function of φ_{M_3}, normalized to the respective experimental upper bound.

Variation of the phases $\varphi_{M_i} (i = 1, 2, 3)$: We comment here on the influence of the phases φ_{M_i} of the gaugino mass parameters M_i on the EDMs. They are other examples for phases, that appear in the MSSM, too. Compared to the results from the previously discussed phases

φ_1, φ_2 and φ_{A_t}, the gaugino phases do not lead to more stringent constraints nor add new effects on the EDMs.

The phase φ_{M_3}, that arises in the stop and gluino sector, does not contribute to the electron EDM. Its contributions to the neutron and Mercury EDM are of the same size as those arising from φ_{A_t}, as can be inferred from Fig. 10. It shows the absolute values of the neutron and the Mercury EDMs as a function of φ_{M_3}, normalized to the respective experimental upper bounds. Here and in the following plots, for the neutron EDM results are given in the chiral quark model approach and in the one based on QCD sum rule techniques. For the Mercury EDM the presented results are obtained for two different values of the Schiff moment, $d_{\rm Hg}^{\rm I}[S]$ and $d_{\rm Hg}^{\rm IV}[S]$, as defined in [69, 81].

The phase φ_{M_2} plays a role in the chargino sector, just as the phase of the effective μ

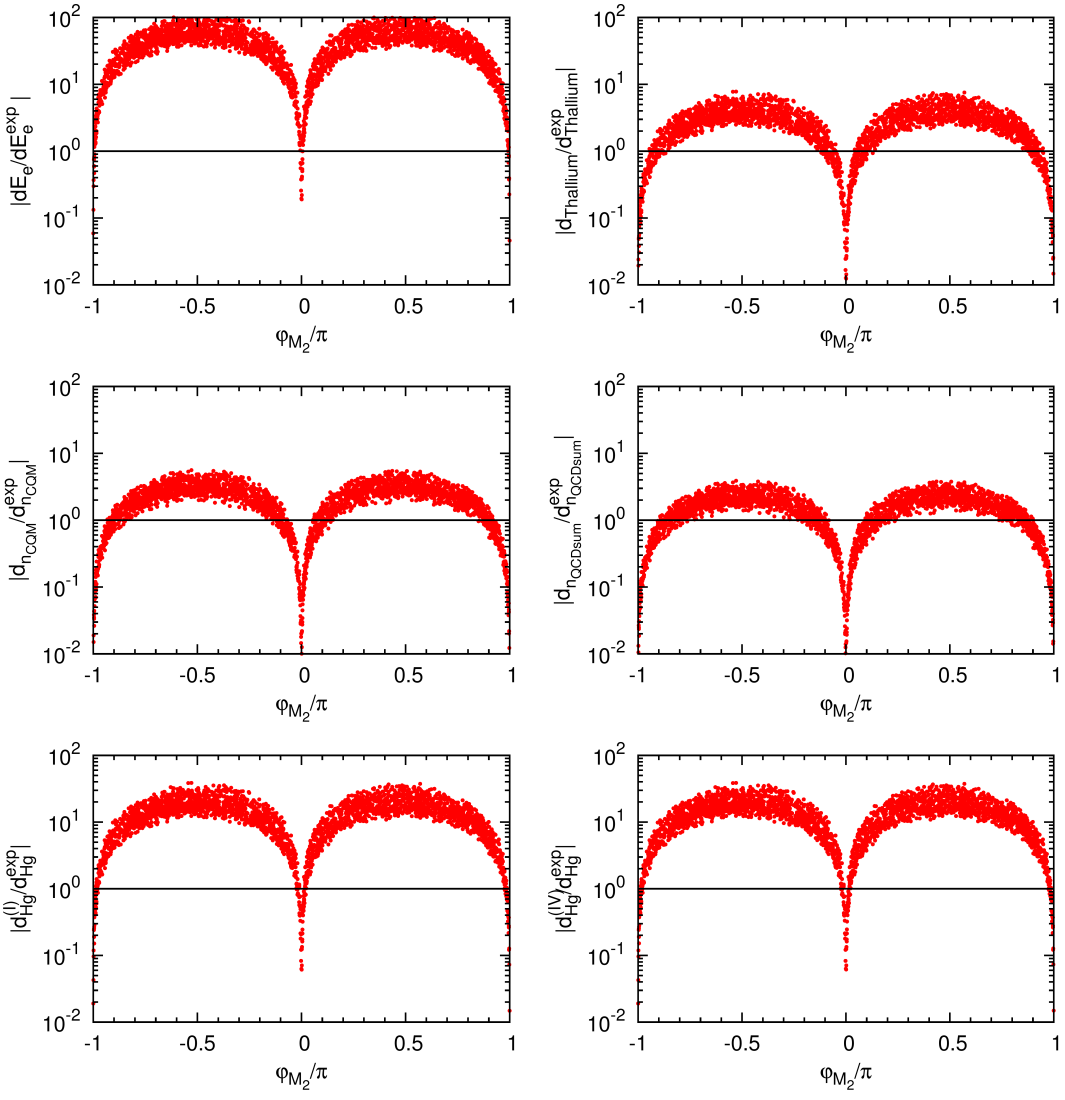

Figure 11: Absolute values of the electron (upper left), Thallium (upper right), neutron (middle) and Mercury (lower) EDMs as a function of φ_{M_2}, normalized to the respective experimental upper bound.

parameter, encoded in φ_1. The sizes of the EDMs due to φ_{M_2} can therefore be expected to be of the same order as those due to φ_1. This is confirmed by the plots given in Fig. 11, which show the absolute values of the electron, Thallium, neutron and Mercury EDMs as a function of φ_{M_2}, normalized to the respective experimental upper bounds. Since the phase φ_{M_2} has only a marginal effect on the Higgs sector, the compatibility of the Higgs data is not affected by φ_{M_2} and no gap around $\pm\pi/2$ arises as in the results for non-zero φ_1, *cf.* Fig. 9.

Finally, the phase φ_{M_1} arises in the neutralino sector and therefore only gives contributions to diagrams that involve neutralinos in the loops. The generated EDMs are smaller than the ones for a non-vanishing φ_{M_2}, *cf.* Fig. 12. The phase φ_{M_1} therefore does not lead to more stringent constraints on the CP-violating NMSSM as the ones that have already been discussed above.

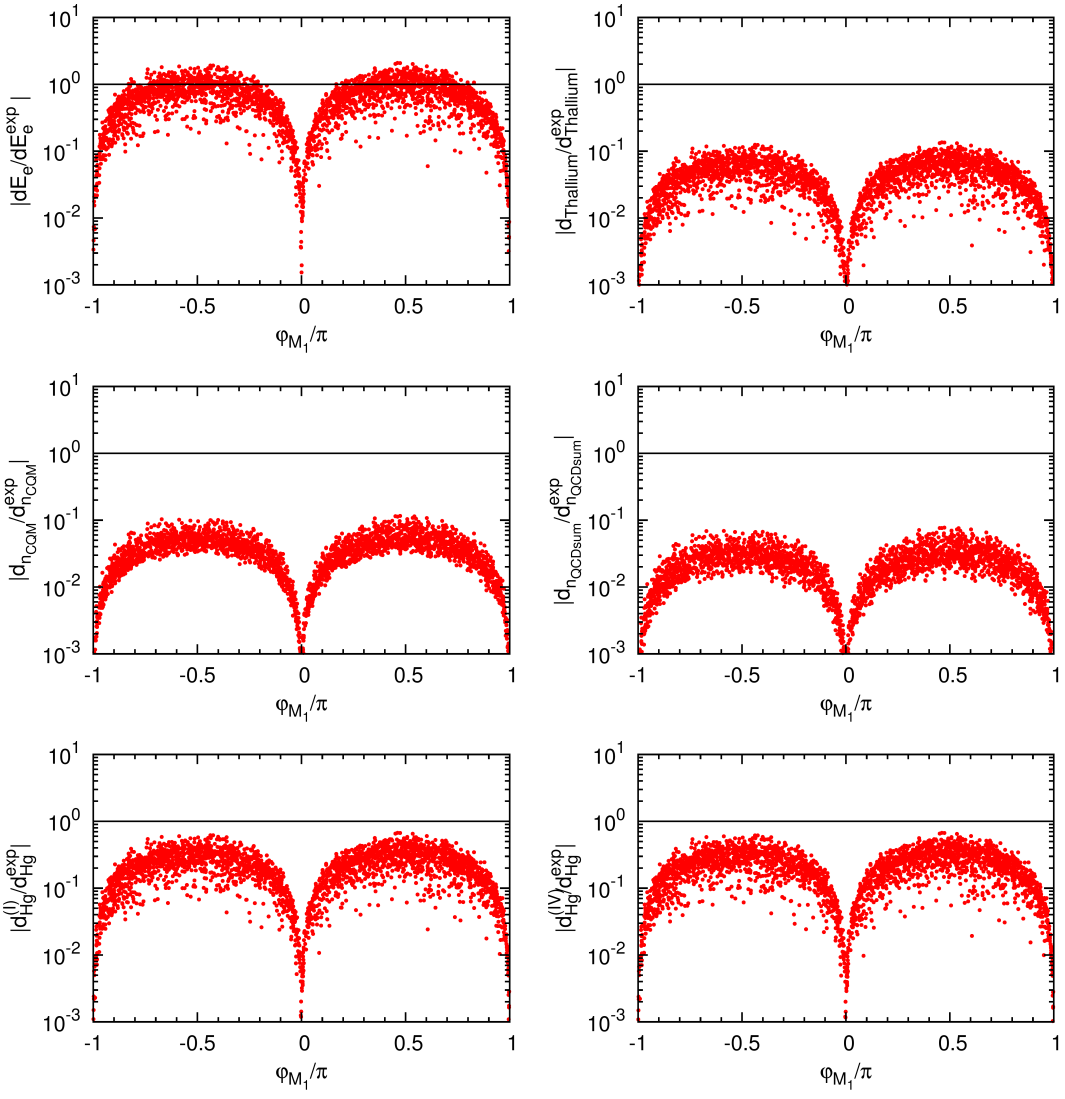

Figure 12: Absolute values of the electron (upper left), Thallium (upper right), neutron (middle) and Mercury (lower) EDMs as a function of φ_{M_1}, normalized to the respective experimental upper bound.

4.2 Enlarged NMSSM Parameter Space

We now turn to the discussion of the EDMs in an enlarged NMSSM parameter space. While the previous scan focused on NMSSM regions that lead to an overall light Higgs mass spectrum with good discovery prospects for all Higgs bosons, we here cover a large part of the NMSSM parameter space. In particular we also allow now for large values of $\tan\beta$ and cover the whole allowed space of λ and κ while taking care of the perturbativity constraint

$$\sqrt{|\lambda|^2 + |\kappa|^2} < 0.7 \; . \tag{4.24}$$

Additionally, we vary the effective μ parameter in a large range. In summary, our scan covers

$$1 \leq \tan\beta \leq 30 \; , \qquad |\lambda| \leq 0.7 \; , \qquad |\kappa| \leq 0.7 \; , \qquad |\mu_{\rm eff}| \leq 1 \text{ TeV} \; . \tag{4.25}$$

The ranges of the remaining parameters are the same as given in Eqs. (4.19)-(4.23). And we again checked for the compatibility with the lower bound on the charged Higgs mass [86] and the exclusion limits on the SUSY particle masses [86–89]. We now also have scenarios where the lightest of the mostly CP-even-like Higgs bosons can be SM-like.

Variation of φ_2: For the scenarios of the large scan we show the results for the EDMs compared to the experimental values in Fig. 13. They are plotted for the electron, the Thallium, the neutron and the Mercury EDM. We have only varied the NMSSM specific phase φ_2 and set all other complex phases to zero. The comparison with the results of the Natural NMSSM in Fig. 5 shows, that more parameter sets now lead to EDMs that exceed the experimental limits. This is particularly striking for the neutron EDM, where the EDMs can be up to a factor of 20 larger. At the same time we have more EDMs with very small values, in particular in the case of large CP-violating phases. The orange points indicate the results for $\tan\beta$ values below 5, while red ones refer to larger $\tan\beta$ values. This shows the strong influence of the $\tan\beta$ parameter on the size of the EDMs. Larger $\tan\beta$ values lead to larger EDMs and vice versa. This is in accordance with the findings of Refs. [64, 90]. Note, finally that Fig. 13 and all subsequent figures of this subsection of course contain the subspace of the Natural NMSSM. As we scan here, however, over a larger parameter space the distribution of the points may not be exactly the same as in the corresponding figures for the Natural NMSSM.

In the enlarged scan, not only the electron EDM, but now also the neutron and Mercury EDMs can lead to stringent constraints on the parameter space. Otherwise, the investigation of the individual contributions shows the same pattern as in the Natural NMSSM subspace. Only the sign of the various contributions is not related to the sign of the phases as clearly any more as *e.g.* in Fig. 6.

Variation of φ_{A_t}: The effect of a non-vanishing MSSM-like phase φ_{A_t} is shown in Fig. 14. Apart from the neutron EDM based on the CQM approach all EDMs display enhancements, sometimes by up to a factor of 50 for the maximal values, due to the large parameter space. This is in particular the case for small phase values, $|\varphi_{A_t}| \lesssim 0.25\ \pi$, and large values of $\tan\beta$, where now all EDMs contribute to the exclusion bounds.

The individual features of the EDMs as discussed already for the Natural NMSSM, do not change.

Variation of φ_1: Finally, we show the constraints arising from a non-vanishing phase φ_1. The enlargement of the parameter space leads to an increase of the maximal values of all EDMs by about a factor of 10, *cf.* Fig. 15. The investigation of the EDMs shows, that for the variation of φ_1 they are very sensitive to the value of $\tan\beta$. This can be inferred from Fig. 15 where the

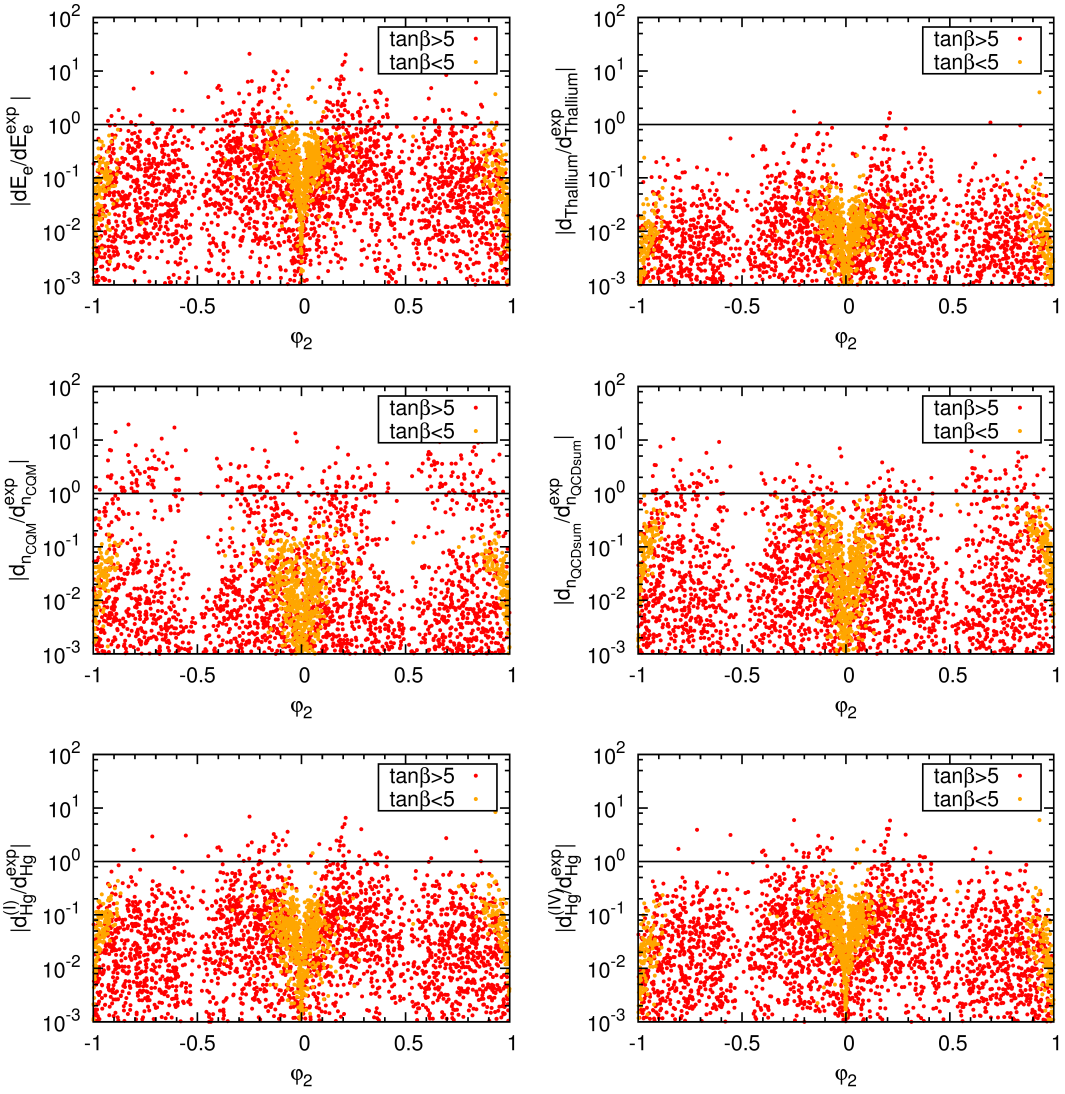

Figure 13: Large parameter scan: Absolute values of the electron (upper left), Thallium (upper right), neutron (middle) and Mercury (lower) EDMs as a function of φ_2, normalized to the respective experimental upper bound; orange: $\tan\beta < 5$, red: $\tan\beta > 5$.

results for $\tan\beta < 5$ are indicated by the orange and those for $\tan\beta > 5$ by the red colour. Overall, the non-vanishing phase φ_1 leads to the strongest constraints on EDMs. This is mainly due to the MSSM-specific CP violation from a complex μ parameter.

We also checked explicitly the behaviour of the EDMs with increasing SUSY particle masses. As expected we observe a decoupling behaviour, *i.e.* the EDMs decrease with increasing SUSY particle masses in the loops.

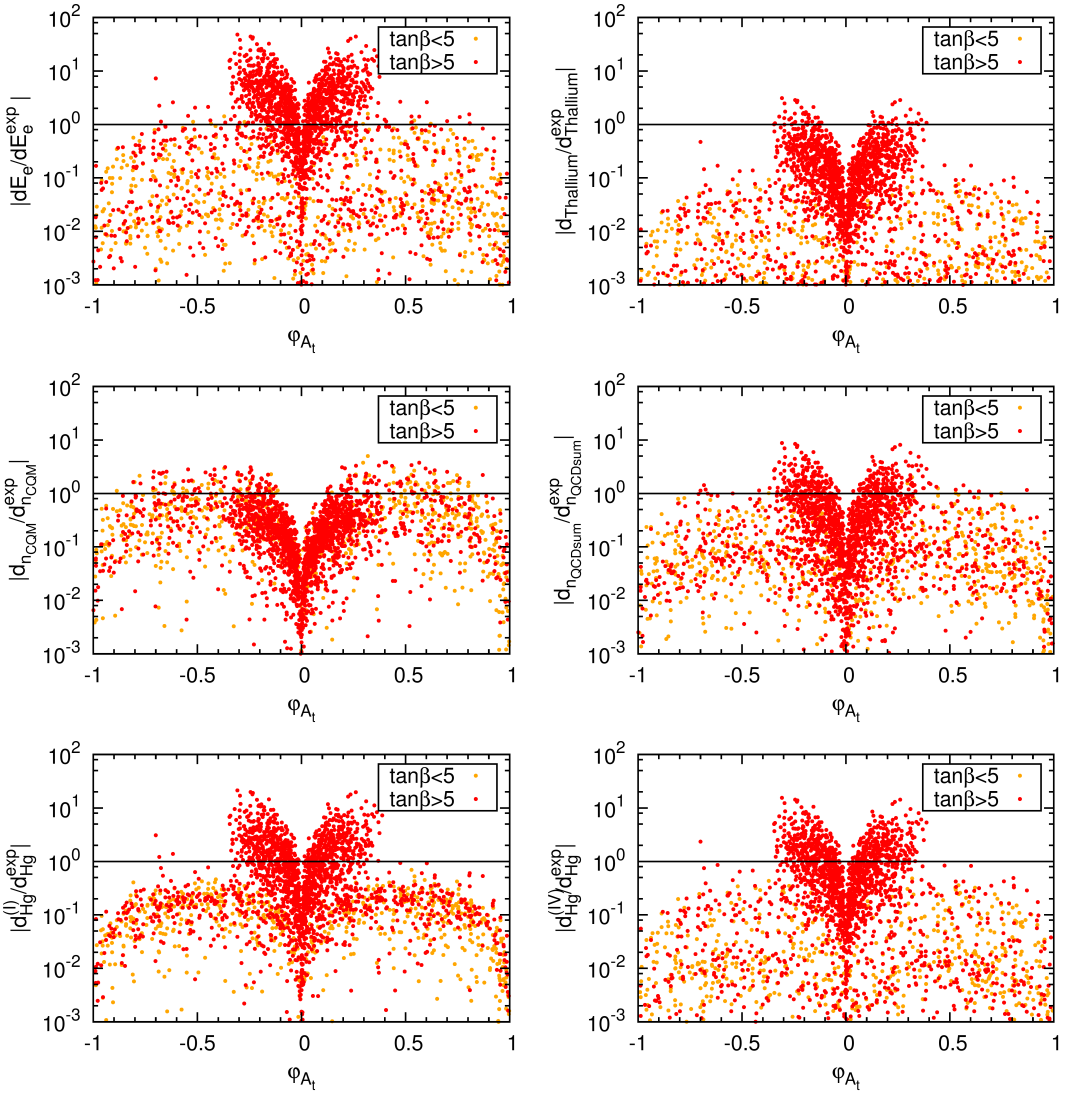

Figure 14: Same as Fig. 13, but for the variation of φ_{A_t}. All other CP-violating phases are set to zero.

5 Phenomenological Higgs Analysis

The explicit verification of CP violation at the LHC is a non-trivial task and requires high luminosities [91]. For the measurement of CP violation, observables can be constructed that are sensitive to CP-violating effects in the Higgs couplings to gauge bosons and fermions.[9] While the Higgs couplings to massive gauge bosons project on the CP-even component of the Higgs state, the fermionic couplings have the advantage to democratically couple to the CP-even and CP-odd components of the Higgs bosons. The individual signal rates, on the other hand, do not allow for conclusions on CP violation, since specific parameter configurations in the CP-conserving NMSSM can lead to the same rates as in the CP-violating case within the experimental errors.

[9]For a comprehensive list of the relevant literature, see *e.g.* [91, 92] and references therein, complemented by recent investigations in [93–113].

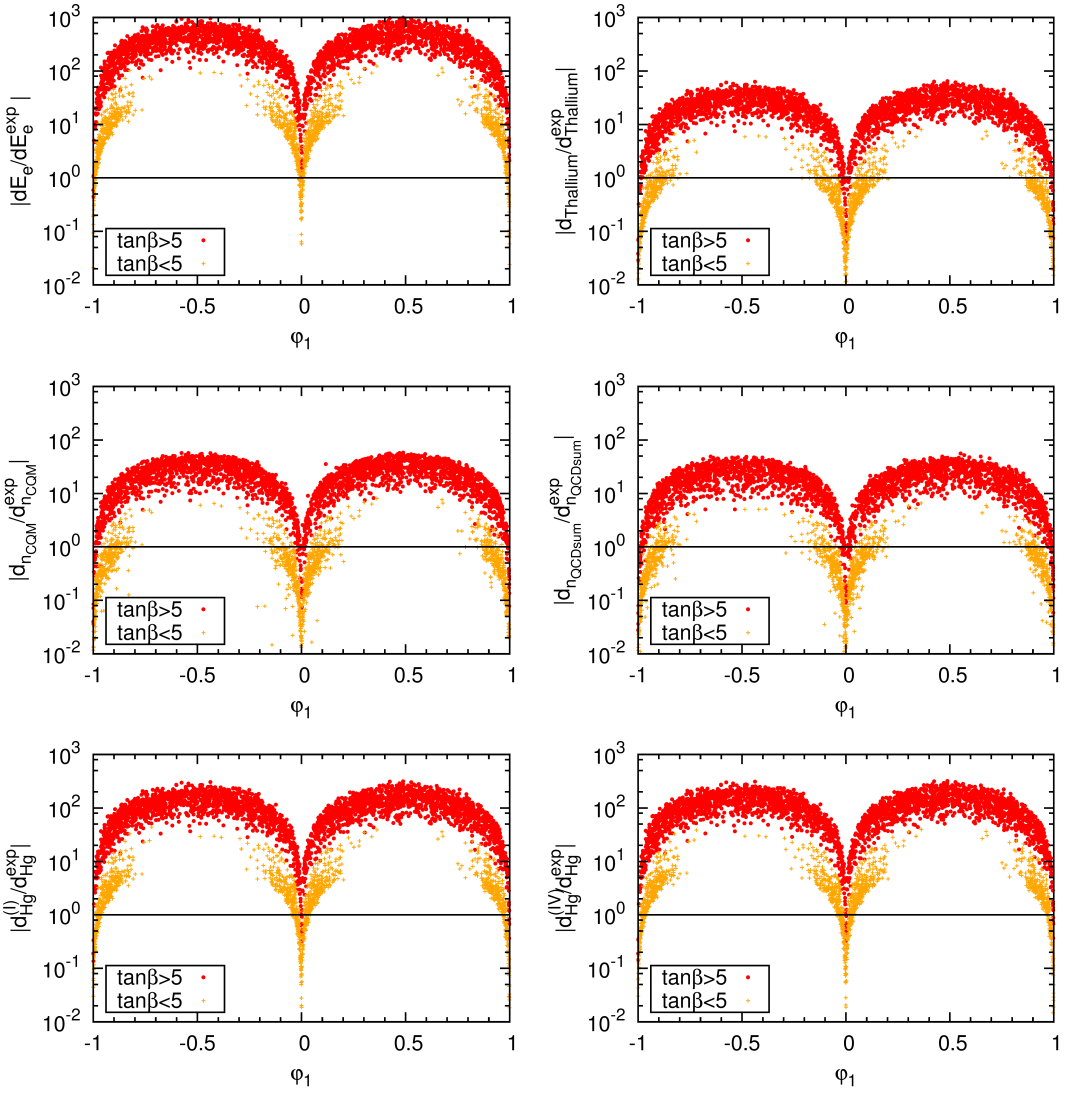

Figure 15: Same as Fig. 13, but for the variation of φ_1. All other CP-violating phases are set to zero.

Also the superposition of rates stemming from CP-odd and CP-even Higgs bosons, that are close in mass, can mimic CP-violating effects. The simultaneous measurement of Higgs decay rates, however, that require a CP-even, respectively, a CP-odd component, allow for conclusions on CP violation.

In the following two subsections we will discuss possible prospects for accessing CP violation in two different approaches. These are on the one hand the combined measurement of signal rates and on the other hand the exploitation of decays into fermion pairs.

5.1 Hints towards CP violation in Higgs decays involving a Z boson

One possibility to pin down CP violation in the Higgs sector is the observation of a combination of decays that is not allowed in CP-conserving scenarios. If a new scalar resonance is discovered there are several decays that offer insights on its CP nature. For example if the new resonance

H' decays into a pair of vector bosons, it has to have a CP-even admixture. Furthermore one can make use of the knowledge that the SM-like Higgs boson at 125 GeV is mostly CP-even. Hence, the decay $H' \to hh$ is also an indication for a large CP-even component of H'. However, if at the same time $H' \to hZ$ can be observed, H' must feature a CP-odd component as well. In short, if we observe

$$\begin{aligned} & H' \to ZZ \quad \text{or} \quad H' \to hh \quad && \widehat{=} \quad && \mathrm{CP}_{H'} = +1 \\ \text{and} \quad & H' \to Zh && \widehat{=} && \mathrm{CP}_{H'} = -1 \end{aligned} \tag{5.26}$$

at the same time this proves CP violation in the Higgs sector.[10]

To illustrate this idea we present an example scenario, taken from the scan we performed with NMSSMCALC as described in Sec. 4. The parameters of the Higgs sector are given by[11]:

$$\begin{aligned} & |\lambda| = 0.635\,, \quad |\kappa| = 0.288\,, \quad |A_\kappa| = 210.70\,\text{GeV}\,, \quad |\mu_{\text{eff}}| = 178.65\,\text{GeV}\,, \\ & \varphi_1 = 0\,, \quad \varphi_2 = 0.0119\,\pi\,, \quad \varphi_{A_\lambda} = 0.0037\,\pi\,, \quad \varphi_{A_\kappa} = 0.983\,\pi\,, \\ & \tan\beta = 1.88\,, \quad M_{H^\pm} = 392.9\,\text{GeV}\,. \end{aligned} \tag{5.27}$$

The other input parameters are

$$\begin{aligned} & m_{\tilde{u}_R,\tilde{c}_R} = m_{\tilde{d}_R,\tilde{s}_R} = m_{\tilde{Q}_{1,2}} = m_{\tilde{L}_{1,2}} = m_{\tilde{e}_R,\tilde{\mu}_R} = 3\ \text{TeV}\,,\ m_{\tilde{t}_R} = 844\,\text{GeV}\,, \\ & m_{\tilde{Q}_3} = 844\,\text{GeV}\,,\ m_{\tilde{b}_R} = 3\,\text{TeV}\,,\ m_{\tilde{L}_3} = 1751\,\text{GeV}\,,\ m_{\tilde{\tau}_R} = 1751\,\text{GeV}\,, \\ & |A_{u,c,t}| = 603\,\text{GeV}\,,\ |A_{d,s,b}| = 16\,\text{GeV}\,,\ |A_{e,\mu,\tau}| = 1086\,\text{GeV}\,, \\ & |M_1| = 764\,\text{GeV},\ |M_2| = 756\,\text{GeV}\,,\ |M_3| = 2650\,\text{GeV}\,, \\ & \varphi_{A_{u,c,t}} = \pi\,,\ \varphi_{A_{d,s,b}} = \varphi_{A_{e,\mu,\tau}} = \varphi_{M_1} = \varphi_{M_2} = \varphi_{M_3} = 0\,. \end{aligned} \tag{5.28}$$

The resulting Higgs spectrum is relatively light,

$$M_{H_1} \approx 104\,\text{GeV}\,, \qquad M_{H_2} \approx 126.4\,\text{GeV}\,, \qquad M_{H_3} \approx 258\,\text{GeV}\,, \tag{5.29}$$

$$M_{H_4} \approx 401\,\text{GeV}\,, \qquad M_{H_5} \approx 405\,\text{GeV}\,. \tag{5.30}$$

Possible candidates for H' are either H_3, H_4 or H_5. However, the two heavy mass eigenstates are very close in mass, so that their individual signals cannot be disentangled. In most scenarios of the CP-conserving case one of the heavy mass eigenstates is CP-even and the other CP-odd. But since it is impossible to tell whether the decay of H_4 or H_5 is observed, no conclusion about CP violation can be drawn. This leaves us with $H' = H_3$. For H_3 both the decay into a pair of vector bosons as well as the decay into a Z boson and the SM-like Higgs boson H_2 are sizeable,

$$\mathrm{BR}(H_3 \to ZH_2) = 5.7\%\,, \quad \mathrm{BR}(H_3 \to ZZ) = 11.8\%\,, \quad \mathrm{BR}(H_3 \to WW) = 27.5\%\,. \tag{5.31}$$

These decays can only be observed if the production cross section for H_3 is sufficiently large. At $\sqrt{s} = 13$ TeV the production cross section through gluon fusion at next-to-next-to-leading order[12] is $\sigma^{13\text{TeV}}_{ggH_3} = 211.2\,\text{fb}$, which is not particularly large for a Higgs boson of this mass. The reason is the suppression of the effective coupling of H_3 to a pair of gluons due to the large singlet admixture to the mass eigenstate. In Table 1 we list the obtained signal rates for several

[10] For a recent investigation in the complex 2-Higgs-Doublet Model, see [114].

[11] Note, that φ_{A_λ} and φ_{A_κ} are strictly speaking not input parameters, but derived quantities, determined via the tadpole conditions.

[12] The cross section has been calculated with a private version of HIGLU [115], that has been adapted to the complex NMSSM.

t

$\sigma(ggH_3)\ \mathrm{BR}\big(H_3 \to ZZ\big)$	24.8 fb
$\sigma(ggH_3)\ \mathrm{BR}\big(H_3 \to WW\big)$	58.1 fb
$\sigma(ggH_3)\ \mathrm{BR}\big(H_3 \to H_2 Z\big)$	12.1 fb
$\sigma(ggH_3)\ \mathrm{BR}\big(H_3 \to H_2 Z \to (bb)Z\big)$	5.5 fb
$\sigma(ggH_3)\ \mathrm{BR}\big(H_3 \to H_2 Z \to (\gamma\gamma)Z\big)$	0.04 fb
$\sigma(ggH_3)\ \mathrm{BR}\big(H_3 \to H_2 Z \to (ZZ)Z\big)$	0.45 fb
$\sigma(ggH_3)\ \mathrm{BR}\big(H_3 \to H_2 Z \to (WW)Z\big)$	3.5 fb
$\sigma(ggH_3)\ \mathrm{BR}\big(H_3 \to H_1 Z\big)$	76.0 fb
$\sigma(ggH_3)\ \mathrm{BR}\big(H_3 \to H_1 Z \to (bb)Z\big)$	66.0 fb
$\sigma(ggH_3)\ \mathrm{BR}\big(H_3 \to H_1 Z \to (\gamma\gamma)Z\big)$	0.04 fb
$\sigma(ggH_3)\ \mathrm{BR}\big(H_3 \to H_1 Z \to (ZZ)Z\big)$	0.06 fb
$\sigma(ggH_3)\ \mathrm{BR}\big(H_3 \to H_1 Z \to (WW)Z\big)$	0.65 fb
$\sigma(ggH_1)\ \mathrm{BR}\big(H_1 \to ZZ\big)$	1.53 fb

Table 1: Signal rates for H_3 production in gluon fusion at $\sqrt{s} = 13$ TeV with subsequent decay into various final states.

final states. The rates in the vector boson final states ZZ and WW are with 24.8 fb and 58.1 fb of moderate size. For the final state ZH_2 the signal only amounts to 12.1 fb. If the decay of the SM-like H_2 is taken into account as well the overall signal becomes rather small. The decay of H_3 into a Z boson and H_1, on the other hand yields a signal rate of 76 fb. Together with the decay of the lightest Higgs boson into a pair of Z bosons, which establishes a CP-even admixture to H_1, this could also be used to search for CP violation in the Higgs sector. The signals are rather small though so that the experimental observation will be challenging.

Note that in this scenario the EDM bounds are respected. As we observed in Sec. 4, this is not uncommon for scenarios that feature $\varphi_2 \neq 0$ and $\varphi_1 = 0$.

5.2 CP violation in the Higgs to $\tau^+\tau^-$ decays

In [103, 116–118] and [94] the possibility to make use of the $\tau^+\tau^-$ decay mode for the determination of the CP properties of a Higgs boson has been suggested. We therefore investigate here the coupling of Higgs bosons to a τ pair. If a mass eigenstate H_i is an admixture of CP-even and CP-odd components, it can feature both a scalar coupling (denoted by c_τ^S) and a pseudoscalar coupling (denoted by c_τ^P). The corresponding term in the Lagrangian reads

$$\mathcal{L}_{H_i\tau\tau} = -g_\tau\, \tau^+ \left(c_\tau^S + i c_\tau^P \gamma_5\right) \tau^-\, H_i \qquad \text{with } g_\tau = \frac{m_\tau}{v} \tag{5.32}$$

$$= -g_\tau \sqrt{(c_\tau^S)^2 + (c_\tau^P)^2}\ \tau^+ \left(\cos\phi_i + i \sin\phi_i\, \gamma_5\right) \tau^-\, H_i \quad \text{with } \tan\phi_i = \frac{c_\tau^P}{c_\tau^S}\,. \tag{5.33}$$

In the second line we followed [103,119] and introduced the CP-violating angle ϕ_i which parametrizes the CP-mixing of the Higgs boson H_i which couples to the τ. For a CP-even Higgs boson

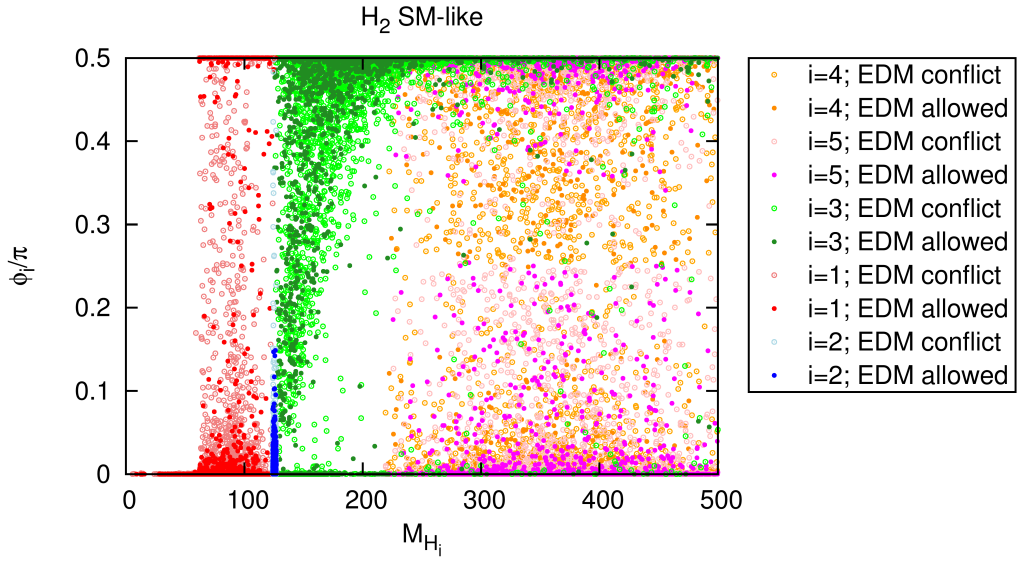

Figure 16: The phase ϕ_i, which measures the CP violation in the $H_i\tau^+\tau^-$ coupling, as a function of the mass of the Higgs boson H_i. Only scenarios that feature H_2 as the SM-like Higgs boson with a mass of 125 GeV are included. Light colored open points are in conflict with the EDM bounds, whereas dark colored full points respect the bounds.

$\phi_i = 0$, and for a CP-odd one $\phi_i = \pi/2$. Figure 16 shows ϕ_i plotted against the mass of the respective Higgs boson. We included all points of the previously described scans that feature the next-to-lightest Higgs boson as the 125 GeV Higgs state. The light colored open points indicate conflict with the EDM constraints, while dark colored full points respect the EDM constraints. Figure 16 shows that H_1 and H_2 couple mostly scalar-like to the τ pair, whereas H_3 features a pseudoscalar-like coupling in most cases. For the heavier Higgs states no such tendency can be observed. Especially for the three heavier Higgs states there are points that display CP violation in the $H_i\tau^+\tau^-$ coupling and that are not in conflict with the EDM bounds.

In the following we investigate by which phases of the input parameters these CP-violating effects in the $H_i\tau^+\tau^-$ coupling can be generated. Figure 17 shows the phase ϕ_i plotted versus several phases of the input parameters, namely φ_1 (upper left), φ_2 (upper right), φ_{A_t} (lower left) and $\varphi_1 = \varphi_2$ (lower right). Even relatively small phases of φ_1 and φ_2 can generate considerable CP violation in the $H_i\tau^+\tau^-$ couplings that should be accessible in the experiment. This is due to CP violation already at tree level in the Higgs sector, that can occur if solely φ_1 or φ_2 are set to non-trivial values. As we already saw earlier the EDM bounds are exceeded, however, if φ_1 takes on non-trivial values, whereas φ_2 leads to scenarios, which respect the bounds. If the CP violation is only induced by loop effects, as it is the case for φ_{A_t} or if φ_1 and φ_2 are chosen equal, hardly any CP-violating effect is visible in the $H_i\tau^+\tau^-$ coupling. The prospects of measuring such a small CP violation are less good in this case.

6 Conclusions

Supersymmetric theories feature many new sources for CP violation. In particular in the NMSSM, CP violation can already be induced at tree level in the Higgs sector. The upper bounds on the EDMs, on the other hand, pose stringent constraints on possible CP-violating

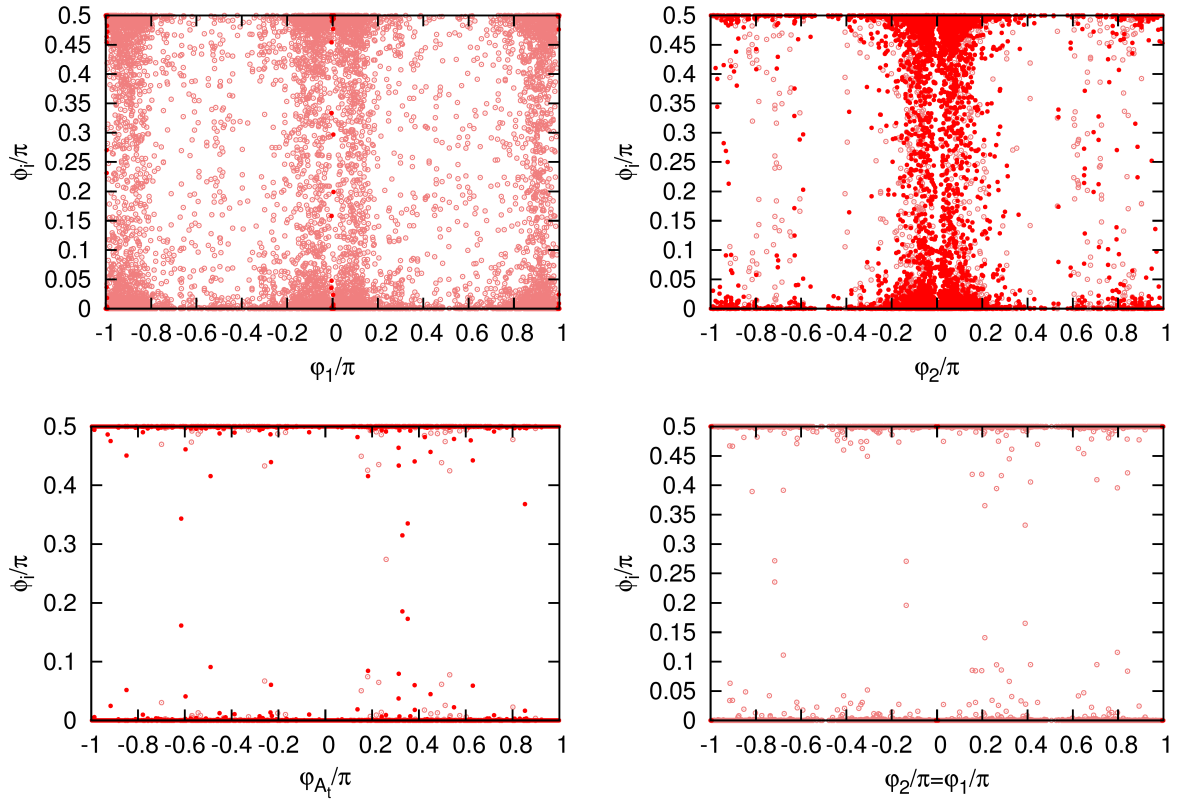

Figure 17: The angle ϕ_i as a function of various phases of the input parameters. All other phases are set to zero. Light colored open points are in conflict with the EDM constraints, whereas dark colored full points respect the bounds.

phases. We have investigated the allowed ranges for CP-violating phases in the NMSSM by taking into account the current limits on EDMs and the latest Higgs data from the LHC. On the one hand the phase $\varphi_1 - \varphi_2$, which induces the tree-level CP violation in the Higgs sector, is of interest. On the other hand radiative corrections to the Higgs masses are indispensable to achieve the measured mass value of 125 GeV for the SM-like Higgs boson. In particular the top/stop sector, which delivers the dominant Higgs mass corrections, introduces the additional phase φ_{A_t}. Furthermore the phase φ_1 appears on its own (not in combination with φ_2) in the stop sector and also enters in the chargino sector.

Our analysis has shown that the EDMs induced by the NMSSM specific phase φ_2, that appears already at tree level in the NMSSM Higgs sector in contrast to the MSSM, leads to small contributions to the EDMs. In this case, non-trivial CP-violating phases can still be compatible with the EDMs. The most stringent constraints on the phases are then due to the LHC Higgs data, as the possible large CP admixture in the 125 GeV Higgs boson leads to signal rates that are not compatible with the experiment any more. On the other hand chargino contributions to the EDMs through a complex phase of the effective μ parameter generate EDMs that are above the experimental constraints. The EDM contributions stemming from a non-vanishing phase φ_{A_t} can be important for small values of the phases and large values of $\tan\beta$. Otherwise, this phase is hardly constrained by the EDMs. Overall, we observe that the induced EDMs are more important for larger values of $\tan\beta$. Finally the phases of the gaugino mass parameters

can induce sizeable EDM contributions. We have also verified, that the CP-violating effects in the EDMs decouple with rising masses of the SUSY particles in the loops as expected.

The experimental verification of CP violation in the Higgs sector is a non-trivial task. Higgs signal rates can be used for the verification of CP violation only in the simultaneous measurement of decay rates requiring a dominantly CP-even, respectively, CP-odd admixture in the Higgs mass eigenstate. We have shown one example where such measurements should be feasible, although the signal rates are challenging. Besides other observables, Higgs decays into fermions provide observables sensitive to CP violation. Taking into account the EDM and LHC Higgs constraints we have shown, that in particular for the three heavier Higgs bosons there are scenarios that display CP violation in the Higgs couplings to tau leptons and are not in conflict with the bounds on the EDMs. Our investigation of the origin of the CP effects has revealed, that CP violation induced by loop effects hardly leads to CP-violating Higgs couplings to fermions. Large CP-violating effects are generated by the CP-violating phases present already at tree level in the NMSSM Higgs sector. While the parameter points for non-vanishing values of φ_1 are to a large extent excluded by the EDM bounds, those for non-trivial φ_2 values respect the EDM constraints. In this case, CP violation in the Higgs couplings to τ leptons may be accessible experimentally.

Acknowledgments

SFK acknowledge partial support from the STFC Consolidated ST/J000396/1 and the European Union FP7 ITN-INVISIBLES (Marie Curie Actions, PITN- GA-2011-289442). The work by RN was supported by the Australian Research Council through the ARC Center of Excellence in Particle Physics at the Terascale. KW has been supported in part by the Graduiertenkolleg "GRK 1694: Elementarteilchenphysik bei höchster Energie und höchster Präzision". The authors thank Rui Santos for helpful discussions.

References

[1] G. Aad *et al.* [ATLAS Collaboration], Phys. Lett. B **716** (2012) 1 [arXiv:1207.7214 [hep-ex]]; G. Aad *et al.* [ATLAS Collaboration], ATLAS-CONF-2012-162.

[2] S. Chatrchyan *et al.* [CMS Collaboration], Phys. Lett. B **716** (2012) 30 [arXiv:1207.7235 [hep-ex]]; S. Chatrchyan *et al.* [CMS Collaboration], CMS-PAS-HIG-12-045.

[3] D.V. Volkov and V.P. Alkulov, Phys. Lett. **B46** (1973) 109; J. Wess and B. Zumino, Nucl. Phys. **B70** (1974) 39; P. Fayet, Phys. Lett. **B64** (1976) 159, Phys. Lett. **B69** (1977) 489, Phys. Lett. **B84** (1979) 416; G.F. Farrar and P. Fayet, Phys. Lett. **B76** (1978) 575; S. Dimopoulos and H. Georgi, Nucl. Phys. **B193** (1981) 150; N. Sakai, Z. Phys. **C11** (1981) 153; E. Witten, Nucl. Phys. **B188** (1981) 513; H.P. Nilles, Phys. Rep. **110** (1984) 1; H.E. Haber and G.L. Kane, Phys. Rep. **117** (1985) 75; M.F. Sohnius, Phys. Rep. **128** (1985) 39; J.F. Gunion and H.E. Haber, Nucl. Phys. **B272** (1986) 1 [Erratum-ibid. **B402** (1993) 567], Nucl. Phys. **B278** (1986) 449; A.B. Lahanas and D.V. Nanopoulos, Phys. Rep. **145** (1987) 1.

[4] For reviews and further references, see: J.F. Gunion, H.E. Haber, G. Kane and S. Dawson, *"The Higgs Hunter's Guide"*, Addison-Wesley, 1990; S.P. Martin, [hep-ph/9709356]; S.

Dawson, [hep-ph/9712464]; M. Gomez-Bock, M. Mondragon, M. Mühlleitner, R. Noriega-Papaqui, I. Pedraza, M. Spira and P. M. Zerwas, J. Phys. Conf. Ser. **18** (2005) 74 [arXiv:hepph/0509077]; M. Gomez-Bock, M. Mondragon, M. Mühlleitner, M. Spira and P. M. Zerwas, [arXiv:0712.2419 [hep-ph]]; A. Djouadi, Phys. Rept. **459** (2008) 1 [hep-ph/0503173].

[5] P. Fayet, Nucl. Phys. **B90** (1975) 104; R. Barbieri, S. Ferrara, C. A. Savoy, Phys. Lett. **B119** (1982) 343; M. Dine, W. Fischler, M. Srednicki, Phys. Lett. **B104** (1981) 199; H. P. Nilles, M. Srednicki, D. Wyler, Phys. Lett. **B120** (1983) 346; J. M. Frere, D. R. T. Jones, S. Raby, Nucl. Phys. **B222** (1983) 11; J. P. Derendinger, C. A. Savoy, Nucl. Phys. **B237** (1984) 307; J. R. Ellis, J. F. Gunion, H. E. Haber, L. Roszkowski, F. Zwirner, Phys. Rev. **D39** (1989) 844; M. Drees, Int. J. Mod. Phys. **A4** (1989) 3635; U. Ellwanger, M. Rausch de Traubenberg, C. A. Savoy, Phys. Lett. **B315** (1993) 331 [hep-ph/9307322], Z. Phys. **C67** (1995) 665 [hep-ph/9502206], Nucl. Phys. **B492** (1997) 21 [hep-ph/9611251]; T. Elliott, S. F. King, P. L. White, Phys. Lett. **B351** (1995) 213 [hep-ph/9406303]; S. F. King, P. L. White, Phys. Rev. **D52** (1995) 4183 [hep-ph/9505326]; F. Franke, H. Fraas, Int. J. Mod. Phys. **A12** (1997) 479 [hep-ph/9512366]; M. Maniatis, Int. J. Mod. Phys. **A25** (2010) 3505 [arXiv:0906.0777 [hep-ph]]; U. Ellwanger, C. Hugonie, A. M. Teixeira, Phys. Rept. **496** (2010) 1 [arXiv:0910.1785 [hep-ph]].

[6] J.E. Kim and H.P. Nilles, Phys. Lett. **B138** (1984) 150.

[7] A. Sakharov, Pisma Zh. Eksp. Teor. Fiz. **5** (1967) 32.

[8] N. Cabibbo, Phys. Rev. Lett. **10** (1963) 531.

[9] M. Kobayashi and T. Maskawa, Prog. Theor. Phys. **49** (1973) 652.

[10] S. Schael *et al.* [ALEPH, DELPHI, L3 and OPAL Collaborations], Eur. Phys. J. C **47** (2006) 547.

[11] S. Moretti and S. Munir, arXiv:1505.00545 [hep-ph].

[12] T. Graf, R. Grober, M. Muhlleitner, H. Rzehak and K. Walz, JHEP **1210** (2012) 122 [arXiv:1206.6806 [hep-ph]].

[13] M. Muhlleitner, D. T. Nhung, H. Rzehak and K. Walz, JHEP **1505** (2015) 128 [arXiv:1412.0918 [hep-ph]].

[14] R. Barbieri, D. Buttazzo, K. Kannike, F. Sala and A. Tesi, Phys. Rev. **D87** (2013) 115018 [arXiv:1304.3670 [hep-ph]].

[15] D. T. Nhung, M. Muhlleitner, J. Streicher and K. Walz, JHEP **1311** (2013) 181 [arXiv:1306.3926 [hep-ph]].

[16] U. Ellwanger, JHEP **1308** (2013) 077 [arXiv:1306.5541 [hep-ph]].

[17] C. Han, X. Ji, L. Wu, P. Wu and J. M. Yang, JHEP **1404** (2014) 003 [arXiv:1307.3790 [hep-ph]].

[18] S. Munir, Phys. Rev. D **89** (2014) 095013 [arXiv:1310.8129 [hep-ph]].

[19] S. F. King, M. Muhlleitner and R. Nevzorov, Nucl. Phys. B **860** (2012) 207 [arXiv:1201.2671 [hep-ph]].

[20] S. F. King, M. Muhlleitner, R. Nevzorov and K. Walz, Nucl. Phys. B **870** (2013) 323 [arXiv:1211.5074 [hep-ph]].

[21] S. F. King, M. Muhlleitner, R. Nevzorov and K. Walz, Phys. Rev. D **90** (2014) 9, 095014 [arXiv:1408.1120 [hep-ph]].

[22] J. Cao, D. Li, L. Shang, P. Wu and Y. Zhang, JHEP **1412** (2014) 026 [arXiv:1409.8431 [hep-ph]].

[23] L. Wu, J. M. Yang, C. P. Yuan and M. Zhang, Phys. Lett. B **747** (2015) 378 [arXiv:1504.06932 [hep-ph]].

[24] D. Buttazzo, F. Sala and A. Tesi, arXiv:1505.05488 [hep-ph].

[25] J. Baglio, C. O. Krauss, M. Muhlleitner and K. Walz, arXiv:1505.07125 [hep-ph].

[26] U. Ellwanger, Phys. Lett. B **303** (1993) 271 [hep-ph/9302224].

[27] T. Elliott, S. F. King and P. L. White, Phys. Lett. B **305** (1993) 71 [hep-ph/9302202].

[28] T. Elliott, S. F. King and P. L. White, Phys. Lett. B **314** (1993) 56 [hep-ph/9305282].

[29] T. Elliott, S. F. King and P. L. White, Phys. Rev. D **49** (1994) 2435 [hep-ph/9308309].

[30] P. N. Pandita, Z. Phys. **C59** (1993) 575.

[31] P. N. Pandita, Phys. Lett. B **318** (1993) 338.

[32] U. Ellwanger and C. Hugonie, Phys. Lett. B **623** (2005) 93 [hep-ph/0504269].

[33] G. Degrassi and P. Slavich, Nucl. Phys. B **825** (2010) 119 [arXiv:0907.4682 [hep-ph]].

[34] F. Staub, W. Porod and B. Herrmann, JHEP **1010** (2010) 040 [arXiv:1007.4049 [hep-ph]].

[35] K. Ender, T. Graf, M. Muhlleitner and H. Rzehak, Phys. Rev. D **85** (2012) 075024 [arXiv:1111.4952 [hep-ph]].

[36] M. D. Goodsell, K. Nickel and F. Staub, Phys. Rev. D **91** (2015) 035021 [arXiv:1411.4665 [hep-ph]].

[37] S. W. Ham, J. Kim, S. K. Oh and D. Son, Phys. Rev. D **64** (2001) 035007 [hep-ph/0104144].

[38] S. W. Ham, S. H. Kim, S. K. OH and D. Son, Phys. Rev. D **76** (2007) 115013 [arXiv:0708.2755 [hep-ph]].

[39] S. W. Ham, S. K. Oh and D. Son, Phys. Rev. D **65** (2002) 075004 [hep-ph/0110052].

[40] S. W. Ham, Y. S. Jeong and S. K. Oh, hep-ph/0308264.

[41] K. Funakubo and S. Tao, Prog. Theor. Phys. **113** (2005) 821 [hep-ph/0409294].

[42] K. Cheung, T. J. Hou, J. S. Lee and E. Senaha, Phys. Rev. D **82** (2010) 075007 [arXiv:1006.1458 [hep-ph]].

[43] M. Muhlleitner, D. T. Nhung and H. Ziesche, arXiv:1506.03321 [hep-ph].

[44] U. Ellwanger, J. F. Gunion, and C. Hugonie, JHEP **0502** (2005) 066 [hep-ph/0406215].

[45] U. Ellwanger and C. Hugonie, Comput. Phys. Commun. **175** (2006) 290 [hep-ph/0508022].

[46] U. Ellwanger and C. Hugonie, Comput. Phys. Commun. **177** (2007) 399 [hep-ph/0612134].

[47] B. Allanach, Comput. Phys. Commun. **143** (2002) 305 [hep-ph/0104145].

[48] B. Allanach, P. Athron, L. C. Tunstall, A. Voigt, and A. Williams, Comput. Phys. Commun. **185** (2014) 2322 [1311.7659 [hep-ph]].

[49] J. Baglio et al., EPJ Web Conf. **49**, 12001 (2013).

[50] J. Baglio, R. Grober, M. Muhlleitner, D. T. Nhung, H. Rzehak, M. Spira, J. Streicher and K. Walz, Comput. Phys. Commun. **185** (2014) 12, 3372 [arXiv:1312.4788 [hep-ph]].

[51] P. Athron, J. h. Park, D. Stöckinger and A. Voigt, Comput. Phys. Commun. **190** (2015) 139 [arXiv:1406.2319 [hep-ph]].

[52] P. Athron, J. h. Park, D. Stöckinger and A. Voigt, arXiv:1410.7385 [hep-ph].

[53] W. Porod, Comput. Phys. Commun. **153** (2003) 275 [hep-ph/0301101].

[54] W. Porod and F. Staub, Comput. Phys. Commun. **183** (2012) 2458, [1104.1573 [hep-ph]].

[55] F. Staub, Comput. Phys. Commun. **182** (2011) 808 [1002.0840 [hep-ph]].

[56] F. Staub, Computer Physics Communications **184** (2013) 1792 [1207.0906 [hep-ph]].

[57] F. Staub, Comput. Phys. Commun. **185** (2014) 1773 [1309.7223 [hep-ph]].

[58] M. D. Goodsell, K. Nickel and F. Staub, Eur. Phys. J. C **75** (2015) 1, 32 [arXiv:1411.0675 [hep-ph]].

[59] F. Staub, P. Athron, U. Ellwanger, R. Grober, M. Muhlleitner, P. Slavich and A. Voigt, arXiv:1507.05093 [hep-ph].

[60] F. Domingo, JHEP **1506** (2015) 052 [arXiv:1503.07087 [hep-ph]].

[61] P. Z. Skands et al., JHEP **0407** (2004) 036 [hep-ph/0311123].

[62] B. Allanach et al., Comput. Phys. Commun. **180** (2009) 8 [0801.0045 [hep-ph]].

[63] T. Ibrahim and P. Nath, Phys. Rev. D **58** (1998) 111301 [Erratum-ibid. D **60** (1999) 099902] [arXiv:hep-ph/9807501]

[64] J. R. Ellis, J. S. Lee and A. Pilaftsis, JHEP **0810** (2008) 049 [arXiv:0808.1819 [hep-ph]].

[65] J. Baron et al. [ACME Collaboration], Science **343** (2014) 269 [arXiv:1310.7534 [physics.atom-ph]].

[66] B. C. Regan, E. D. Commins, C. J. Schmidt and D. DeMille, Phys. Rev. Lett. **88** (2002) 071805.

[67] C. A. Baker, D. D. Doyle, G. Geltenhort, K. Green, M. G. D. van der Grinten, P. G. Harris, P. Iaydijev and S. N. Ivanov *et al.*, Phys. Rev. Lett. **97** (2006) 131801 [hep-ex/0602020].

[68] W. C. Griffith, M. D. Swallows, T. H. Loftus, M. V. Romalis, B. R. Heckel and E. N. Fortson, Phys. Rev. Lett. **102** (2009) 101601.

[69] K. Cheung, T. J. Hou, J. S. Lee and E. Senaha, Phys. Rev. D **84** (2011) 015002 [arXiv:1102.5679 [hep-ph]].

[70] J. Ellis, J. S. Lee and A. Pilaftsis, JHEP **1010** (2010) 049 [arXiv:1006.3087 [hep-ph]].

[71] G. F. Giudice and A. Romanino, Phys. Lett. B **634** (2006) 307 [arXiv:hep-ph/0510197]; Y. Li, S. Profumo and M. Ramsey-Musolf, Phys. Rev. D **78** (2008) 075009 [arXiv:0806.2693 [hep-ph]].

[72] D. A. Dicus, Phys. Rev. D **41** (1990) 999; S. Weinberg, Phys. Rev. Lett. **63** (1989) 2333.

[73] J. Dai, H. Dykstra, R. G. Leigh, S. Paban and D. Dicus, Phys. Lett. B **237** (1990) 216 [Erratum-ibid. B **242** (1990) 547].

[74] I. B. Khriplovich and S. K. Lamoreaux, *CP Violation Without Strangeness* (Springer, New York, 1997).

[75] M. Pospelov and A. Ritz, Annals Phys. **318** (2005) 119.

[76] A. Manohar and H. Georgi, Nucl. Phys. B **234** (1984) 189; R. Arnowitt, J. L. Lopez and D. V. Nanopoulos, Phys. Rev. D **42** (1990) 2423; R. Arnowitt, M. J. Duff and K. S. Stelle, Phys. Rev. D **43** (1991) 3085.

[77] J. R. Ellis and R. A. Flores, Phys. Lett. B **377** (1996) 83.

[78] D. A. Demir, O. Lebedev, K. A. Olive, M. Pospelov and A. Ritz, Nucl. Phys. B **680** (2004) 339.

[79] M. Pospelov and A. Ritz, Phys. Rev. Lett. **83** (1999) 2526; M. Pospelov and A. Ritz, Nucl. Phys. B **573** (2000) 177; M. Pospelov and A. Ritz, Phys. Rev. D **63** (2001) 073015; D. A. Demir, M. Pospelov and A. Ritz, Phys. Rev. D **67** (2003) 015007.

[80] K. A. Olive, M. Pospelov, A. Ritz and Y. Santoso, Phys. Rev. D **72** (2005) 075001.

[81] J. Ellis, J. S. Lee and A. Pilaftsis, JHEP **1102** (2011) 045 [arXiv:1101.3529 [hep-ph]], and references therein.

[82] P. Bechtle, O. Brein, S. Heinemeyer, G. Weiglein, and K. E. Williams, Comput. Phys. Commun. **181** (2010) 138.

[83] P. Bechtle, O. Brein, S. Heinemeyer, G. Weiglein, and K. E. Williams, Comput. Phys. Commun. **182** (2011) 2605.

[84] P. Bechtle et al., Eur. Phys. J. **C74** 2693 (2014) 2693.

[85] P. Bechtle, S. Heinemeyer, O. Stal, T. Stefaniak, and G. Weiglein, Eur. Phys. J. **C74** (2014) 2711.

[86] ATLAS Collaboration, ATLAS-CONF-2013-090; CMS Collaboration, CMS-PAS-HIG-12-052.

[87] G. Aad *et al.* [ATLAS Collaboration], arXiv:1405.7875 [hep-ex]; Eur. Phys. J. C **72** (2012) 2237 [arXiv:1208.4305 [hep-ex]]; Phys. Lett. B **720** (2013) 13 [arXiv:1209.2102 [hep-ex]]; JHEP **1406** (2014) 124 [arXiv:1403.4853 [hep-ex]]; JHEP **1310** (2013) 189 [arXiv:1308.2631 [hep-ex]]; arXiv:1407.0583 [hep-ex]; arXiv:1406.1122 [hep-ex].

[88] G. Aad *et al.* [ATLAS Collaboration], arXiv:1407.0608 [hep-ex].

[89] CMS Collaboration [CMS Collaboration], CMS-PAS-SUS-13-019; CMS-PAS-SUS-13-024; CMS-PAS-SUS-14-011; CMS-PAS-SUS-13-011; CMS-PAS-SUS-13-004; CMS-PAS-SUS-13-014; CMS-PAS-SUS-13-018; CMS-PAS-SUS-13-008; CMS-PAS-SUS-13-013.

[90] S. Abel, S. Khalil and O. Lebedev, Nucl. Phys. B **606** (2001) 151 [hep-ph/0103320].

[91] S. Heinemeyer *et al.* [LHC Higgs Cross Section Working Group Collaboration], arXiv:1307.1347 [hep-ph].

[92] R. M. Godbole, D. J. Miller and M. M. Muhlleitner, JHEP **0712** (2007) 031 [arXiv:0708.0458 [hep-ph]].

[93] A. Djouadi and G. Moreau, Eur. Phys. J. C **73** (2013) 9, 2512 [arXiv:1303.6591 [hep-ph]].

[94] R. Harnik, A. Martin, T. Okui, R. Primulando and F. Yu, Phys. Rev. D **88** (2013) 7, 076009 [arXiv:1308.1094 [hep-ph]].

[95] Y. Sun, X. F. Wang and D. N. Gao, Int. J. Mod. Phys. A **29** (2014) 1450086 [arXiv:1309.4171 [hep-ph]].

[96] I. Anderson *et al.*, Phys. Rev. D **89** (2014) 3, 035007 [arXiv:1309.4819 [hep-ph]].

[97] J. Brod, U. Haisch and J. Zupan, JHEP **1311** (2013) 180 [arXiv:1310.1385 [hep-ph], arXiv:1310.1385].

[98] G. Buchalla, O. Cata and G. D'Ambrosio, Eur. Phys. J. C **74** (2014) 3, 2798 [arXiv:1310.2574 [hep-ph]].

[99] W. Dekens, J. de Vries, J. Bsaisou, W. Bernreuther, C. Hanhart, U. G. Meiner, A. Nogga and A. Wirzba, JHEP **1407** (2014) 069 [arXiv:1404.6082 [hep-ph]].

[100] Y. Chen, A. Falkowski, I. Low and R. Vega-Morales, Phys. Rev. D **90** (2014) 11, 113006 [arXiv:1405.6723 [hep-ph]].

[101] M. J. Dolan, P. Harris, M. Jankowiak and M. Spannowsky, Phys. Rev. D **90** (2014) 7, 073008 [arXiv:1406.3322 [hep-ph]].

[102] F. Demartin, F. Maltoni, K. Mawatari, B. Page and M. Zaro, Eur. Phys. J. C **74** (2014) 9, 3065 [arXiv:1407.5089 [hep-ph]].

[103] S. Berge, W. Bernreuther and S. Kirchner, Eur. Phys. J. C **74** (2014) 11, 3164 [arXiv:1408.0798 [hep-ph]].

[104] R. M. Godbole, D. J. Miller, K. A. Mohan and C. D. White, JHEP **1504** (2015) 103 [arXiv:1409.5449 [hep-ph]].

[105] R. Li and Y. Zhang, arXiv:1410.2120 [hep-ph].

[106] J. Yue, Phys. Lett. B **744** (2015) 131 [arXiv:1410.2701 [hep-ph]].

[107] A. Arbey, J. Ellis, R. M. Godbole and F. Mahmoudi, Eur. Phys. J. C **75** (2015) 2, 85 [arXiv:1410.4824 [hep-ph]].

[108] X. G. He, G. N. Li and Y. J. Zheng, arXiv:1501.00012 [hep-ph].

[109] A. Askew, P. Jaiswal, T. Okui, H. B. Prosper and N. Sato, Phys. Rev. D **91** (2015) 7, 075014 [arXiv:1501.03156 [hep-ph]].

[110] F. Boudjema, R. M. Godbole, D. Guadagnoli and K. A. Mohan, Phys. Rev. D **92** (2015) 1, 015019 [arXiv:1501.03157 [hep-ph]].

[111] W. Altmannshofer, J. Brod and M. Schmaltz, JHEP **1505** (2015) 125 [arXiv:1503.04830 [hep-ph]].

[112] T. V. Zagoskin and A. Y. Korchin, arXiv:1504.07187 [hep-ph].

[113] M. R. Buckley and D. Goncalves, arXiv:1507.07926 [hep-ph].

[114] D. Fontes, J. C. Romo, R. Santos and J. P. Silva, arXiv:1506.06755 [hep-ph].

[115] M. Spira, Nucl. Instrum. Meth. A **389** (1997) 357 [hep-ph/9610350].

[116] S. Berge, W. Bernreuther and J. Ziethe, Phys. Rev. Lett. **100** (2008) 171605 [arXiv:0801.2297 [hep-ph]].

[117] S. Berge and W. Bernreuther, Phys. Lett. B **671** (2009) 470 [arXiv:0812.1910 [hep-ph]].

[118] S. Berge, W. Bernreuther, B. Niepelt and H. Spiesberger, Phys. Rev. D **84** (2011) 116003 [arXiv:1108.0670 [hep-ph]].

[119] S. Berge, W. Bernreuther and H. Spiesberger, Phys. Lett. B **727** (2013) 488 [arXiv:1308.2674 [hep-ph]].